Research

Check for updates

Author for correspondence:
J. Garnier
e-mail: josselin.garnier@polytechnique.edu

Onset of energy equipartition among surface and body waves

L. Borcea[1], J. Garnier[2,3] and K. Sølna[4]

[1]Department of Mathematics, University of Michigan, Ann Arbor, MI, 48109 USA
[2]CMAP, CNRS, Ecole polytechnique, Institut Polytechnique de Paris, 91128 Palaiseau Cedex, France
[3]INRIA, France
[4]Department of Mathematics, University of California at Irvine, Irvine, CA 92697, USA

JG, 0000-0002-3518-4159

We derive a radiative transfer equation that accounts for coupling from surface waves to body waves and the other way around. The model is the acoustic wave equation in a two-dimensional waveguide with reflecting boundary. The waveguide has a thin, weakly randomly heterogeneous layer near the top surface, and a thick homogeneous layer beneath it. There are two types of modes that propagate along the axis of the waveguide: those that are almost trapped in the thin layer, and thus model surface waves, and those that penetrate deep in the waveguide, and thus model body waves. The remaining modes are evanescent waves. We introduce a mathematical theory of mode coupling induced by scattering in the thin layer, and derive a radiative transfer equation which quantifies the mean mode power exchange. We study the solution of this equation in the asymptotic limit of infinite width of the waveguide. The main result is a quantification of the rate of convergence of the mean mode powers toward equipartition.

1. Introduction

The description of energy transfer between surface waves and body waves is of interest in seismology [1,2], ultrasonic inspection [3], manipulation of waves [4] and the development of surface acoustic wave devices like filters, resonators and scanners [5]. Radiative transfer [6] has been used for more than 30 years to describe wave propagation in heterogeneous media like the Earth's crust [1,7–9], biological tissue [10], the atmosphere and

the ocean [11,12]. The mathematical theory of radiative transfer in open space, which involves only body waves, is well established [13–17]. However, the coupling between surface waves propagating along boundaries and body waves remains a challenge [2,18–20] that is particularly relevant to understanding seismic coda, the long tail portion of seismograms. Because surface and body waves probe different parts of the Earth, methods like coda wave interferometry [21,22], passive image interferometry [23,24] and the extraction of Green's functions from cross-correlation of diffuse fields [25–28] rely on understanding the composition of the coda at increasing lapse time. It is expected that the power exchange between the surface and body waves evolves over time and eventually leads to equipartition [17,29,30]. But how does this evolution occur and on what time or propagation distance?

This question has motivated a number of recent studies: In [31], the sensitivity of coda waves to perturbations at different depths and for varying lapse time is studied via numerical simulations in a medium with random fluctuations of the pressure and shear wave velocity modelled by a von Kármán distribution with Hurst index 0.5. In [8], the authors study elastic wave mode coupling in a slab geometry using the Born scattering approximation. The Born approximation is also used in [18] to study elastic waves in a half space. A system of coupled integral equations that model the power exchange between surface and body waves is introduced in [20] using a phenomenological approach. The study in [19] considers acoustic waves in a heterogeneous medium with point scatterers, occupying the half-space. The authors impose an impedance (Robin) boundary condition, which leads to a unique wave mode trapped near the surface, whose penetration depth depends on the impedance condition. This model seeks to mimic the situation in seismology while minimizing the mathematical complexity. Using a phenomenological approach, based on the independent scattering approximation, the analysis in [19] predicts the equipartition of energy between surface and body waves at long lapse times. The mathematical analysis in [32] also uses the acoustic wave equation in the half space, but with a thin randomly inhomogeneous layer at the surface instead of an impedance boundary condition. This thin layer supports guided modes that play the role of surface waves, provided the index of refraction in the thin layer is larger than the one below it. This model makes it possible to describe the power transfer from the surface waves to the radiating modes, which play the role of body waves. However, the reverse power transfer is negligible [32].

In this paper, we propose a two-dimensional waveguide model for studying the back and forth transfer of power between surface and body waves. The waveguide has two perfectly reflecting parallel boundaries at distance D, and contains a thin layer of width d, comparable to the wavelength and much smaller than D, adjacent to the top boundary and filled with a weakly randomly heterogeneous medium. The remaining part of the waveguide is filled with a homogeneous medium, as illustrated in figure 1. The advantage of the waveguide model is that it allows the decomposition of the wave field in a complete, countable set of modes that are either waves that propagate along the axis of the waveguide, or are evanescent waves. Among the propagating waves, a few are trapped within the thin random layer, and play the role of surface waves. The remaining propagating waves are body waves that are supported in the entire waveguide. The number and penetration depth of the surface waves depend on the thickness of the thin layer and the ratio between the indices of refraction in the thin layer and in the background homogeneous medium below it. Hence, this model mimics the situation in seismology with significant flexibility.

We use stochastic asymptotic analysis to analyse the coupling of the modes. The asymptotic parameter $\varepsilon \ll 1$ quantifies the small amplitude of the random fluctuations of the wave speed in the thin layer, and the waves propagate at large, ε-dependent distance, so that mode coupling induced by scattering becomes significant. The result of the asymptotic analysis in the limit $\varepsilon \to 0$ is a new radiative transfer equation that accounts for power exchange between all the modes. We study its solution in the regime $D \gg d$, so that we approach the half-space setting. We prove that an equipartition between surface and body waves is established at very large range[1] (propagation

---

[1] We study the wave propagation at fixed frequency and with large range, which corresponds to long lapse time in the time domain.
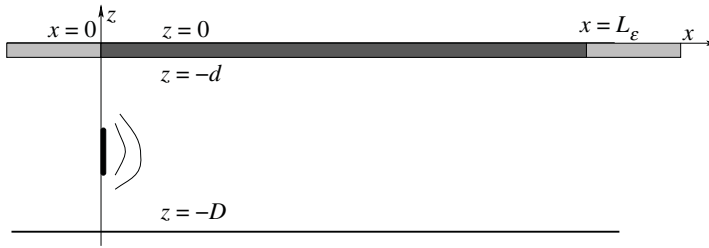
Figure 1. Illustration of the set up in a two-dimensional waveguide with reflecting boundaries at $z = 0$ and $z = -D$. The direction of propagation of the waves is along the x (range) axis. The coordinate z is the cross-range. The random medium with average index of refraction $n > 1$ lies in the subset $(0, L_\varepsilon) \times (-d, 0)$, the thin layer shown with the darkest colour. The medium in $\{\mathbb{R} \setminus (0, L_\varepsilon)\} \times (-d, 0)$ is homogeneous with index of refraction n. The medium in $\mathbb{R} \times (-D, -d)$ is homogeneous with index of refraction 1. The source is supported at $x = 0$, for z between $-D$ and 0.

distance), but the dynamics is multi-scale: there is a quick evolution of the surface mode powers which leads to the establishment of a metastable distribution of power among these modes. This metastable distribution is uniform only under special circumstances, otherwise it depends on the effective coupling coefficients between the surface and body waves. The body mode powers evolve slowly and they modify the metastable distribution of the surface mode powers, until the equilibrium equipartition is reached.

The main result can be summarized as follows: Let N be the number of propagating modes, which includes $N_s \ll N$ surface wave modes and $N_b = N - N_s$ body wave modes, and let $P_j(x)$, $j = 1, \ldots, N$, be their mean powers. The initial power distribution is determined by the source located at the origin of the range coordinate x, but mode coupling redistributes the power as x grows. We consider a smooth covariance function $\mathcal{C}$ of the random fluctuations of the index of refraction in the thin surface layer, and a scaling regime which gives weak backscattering. Therefore, the power redistribution can be described as an evolution problem, i.e. the radiative transfer equation

$$\partial_x P_j(x) = \sum_{l=1}^{N} \Gamma_{jl}^c [P_l(x) - P_j(x)], \quad x > 0, \tag{1.1}$$

with constant $N \times N$ coupling matrix $\boldsymbol{\Gamma}^c = (\Gamma_{jl}^c)_{j,l=1}^N$. This matrix is defined in terms of the covariance $\mathcal{C}$ and the eigenvalues and eigenfunctions of the Sturm–Liouville (Helmholtz) operator $\partial_z^2 + k^2 n_0^2(z)$ in the coordinate $z \in (-D, 0)$, where $n_0(z)$ is the index of refraction in the reference waveguide (without the random fluctuations). The eigenfunctions define the cross-range profiles of the modes.

Using the expression of $\boldsymbol{\Gamma}^c$, we identify and quantify three characteristic range scales on which the mean mode powers evolve:

(1) The shorter scale, that gives the order of x where there is strong coupling among the surface modes, which drives their mean powers towards a metastable distribution.

(2) The intermediate range scale, which defines the order of x where mode coupling results in a slow evolution of both the mean powers of the body modes and the metastable distribution of the mean powers of the surface modes.

(3) The larger scale, which gives the order of x where the mean powers of the body modes evolve towards equipartition. As this occurs, the metastable equilibrium of the surface mode powers also becomes the uniform distribution, so the whole system arrives at a global equipartition with uniform mean mode power distribution.

The paper is organized as follows: We begin in §2 with the set-up. Then we describe in §3 the propagating (surface and body wave) modes and the evanescent modes in the reference

waveguide. These modes form a complete set used to expand the wave field in the randomly perturbed waveguide. The effective dynamics of the random mode amplitudes in the limit $\varepsilon \to 0$ is given in §4. We also give there the radiative transfer equation for the mean mode powers. The main result of the paper, which is the characterization of the evolution of these powers and the convergence to equipartition in the regime with large D/d is in §5. In §6, we present numerical results for large D/d. We end with a summary in §7.

2. Set-up

We consider time-harmonic acoustic waves in a two-dimensional waveguide illustrated in figure 1. The waveguide is in the domain $(x, z) \in \mathbb{R} \times (-D, 0)$, where z is the depth (cross-range) coordinate and the range coordinate x is along the direction of propagation of the waves. The wave field $p(x, z)$ satisfies the Helmholtz equation,

$$\left[\partial_x^2 + \partial_z^2 + k^2 n_\varepsilon^2(x, z) \right] p(x, z) = \delta'(x) f(z), \quad (x, z) \in \mathbb{R} \times (-D, 0), \tag{2.1}$$

with boundary conditions

$$p(x, z = 0) = 0 \quad \text{and} \quad \partial_z p(x, z = -D) = 0, \tag{2.2}$$

and radiation conditions at $|x| \to \infty$. Here k is the wavenumber calculated with the reference wave speed in the homogeneous medium occupying the bottom section $\mathbb{R} \times (-D, -d)$ of the waveguide. The thin layer $\mathbb{R} \times (-d, 0)$, with $0 < d < D$, is filled with a medium whose index of refraction has an average value that is larger than in the bottom section and is randomly fluctuating in the section $x \in (0, L^\varepsilon)$. We will take $D \gg d$ in §5. The model of the index of refraction is

$$n_\varepsilon^2(x, z) = \begin{cases} n^2 + \varepsilon v(x, z) & \text{if } (x, z) \in (0, L_\varepsilon) \times (-d, 0), \\ n^2 & \text{if } (x, z) \in \{\mathbb{R} \backslash (0, L_\varepsilon)\} \times (-d, 0), \\ 1 & \text{otherwise}, \end{cases} \tag{2.3}$$

with constant $n > 1$, so that there are nearly trapped modes in the thin layer, which play the role of surface waves. The fluctuations are modelled in (2.3) by the zero-mean, bounded, stationary in x random process $v(x, z)$, with covariance function

$$\mathcal{C}(x, z, z') = \mathbb{E}[v(x', z) v(x + x', z')]. \tag{2.4}$$

The typical amplitude of the fluctuations is small, as modelled by the small and positive dimensionless parameter ε. As a function of x, the covariance function is assumed to decay fast enough at infinity so that a diffusion-approximation theorem ([33], ch. 6) can be used. Specifically, $\mathcal{C}$ should belong to $L^{1/2}$ as a function of x. The dependence of $\mathcal{C}$ on x is also assumed to be smooth, or equivalently, its Fourier transform with respect to x is assumed to decay fast enough, so that the forward-scattering approximation that we discuss in §4a is valid. A typical example is the Gaussian covariance function (6.2).

The reference length scale is the wavelength $2\pi/k$, and the width d of the thin layer satisfies $kd = O(1)$, so that there is a finite number of surface waves. When $D \gg d$, the waveguide supports a large number of body waves, which is proportional to kD as explained below. We will see that the net scattering effect of the random fluctuations of the index of refraction becomes of order one at range distances of order ε^{-2}, so we consider the interesting case $L_\varepsilon = L/\varepsilon^2$. The fluctuations in (2.3) do not extend beyond the range L_ε, so we can set a radiation boundary condition at $x \to \infty$. We also assume that they are supported at positive range, because we focus attention on the propagation in the forward direction $x > 0$, away from the source modelled by the right-hand side in equation (2.1). This source is localized at $x = 0$ (it is proportional to the derivative of the Dirac $\delta(x)$) and has a transverse profile $f(z)$.

3. Waveguide modes

The stochastic analysis of the net scattering effect of the random medium uses the decomposition of the wave field in the orthonormal $L^2(-D, 0)$ basis of the eigenfunctions $(\phi_j(z))_{j \geq 1}$ of the Sturm–Liouville operator $\partial_z^2 + k^2 n_0^2(z)$, with domain $\{\phi \in H^2(-D, 0) : \phi(0) = \partial_z \phi(-D) = 0\}$ and coefficient

$$n_0^2(z) = \begin{cases} n^2 & \text{if } z \in (-d, 0), \\ 1 & \text{if } z \in (-D, -d). \end{cases} \tag{3.1}$$

This operator has a discrete spectrum $(\lambda_j)_{j \geq 1}$, with simple eigenvalues satisfying

$$\cdots < \lambda_j < \cdots < \lambda_1 < n^2 k^2, \quad \lim_{j \to +\infty} \lambda_j = -\infty. \tag{3.2}$$

The waveguide modes are special solutions of the Helmholtz equation with index of refraction (3.1). They are waves with transverse profile defined by the eigenfunctions, that propagate or decay along the x-axis. Among the propagating modes, we distinguish those that are trapped in the thin layer, and thus model surface waves. The eigenfunctions that define them are described in §3a. The other propagating modes penetrate in the whole cross section of the waveguide, and thus model body waves. The eigenfunctions that define the body and the evanescent waves are described in §3b. The mode wave decomposition in the reference (unperturbed) waveguide is in §3c and the decomposition in the random waveguide is in §3d.

(a) The eigenfunctions that define the surface waves

Here we describe the eigenvalues $(\lambda_j)_{1 \leq j \leq N_s}$ in the spectral interval $(k^2, n^2 k^2)$, and the corresponding eigenfunctions

$$\phi_j(z) = \begin{cases} A_j \sin\left[z\sqrt{k^2 n^2 - \lambda_j}\right], & \text{if } z \in (-d, 0), \\ B_j \cosh\left[(D + z)\sqrt{\lambda_j - k^2}\right], & \text{if } z \in (-D, -d). \end{cases} \tag{3.3}$$

The constants A_j and B_j are related by

$$B_j = -A_j \frac{\sin\left[d\sqrt{k^2 n^2 - \lambda_j}\right]}{\cosh\left[(D - d)\sqrt{\lambda_j - k^2})\right]}, \tag{3.4}$$

so that $\phi_j(z)$ is continuous at $z = -d$, and A_j is defined, up to a sign, using the normalization $\int_{-D}^0 \phi_j(z)^2 \, dz = 1$. The continuity of $\partial_z \phi_j(z)$ at $z = -d$ implies that the eigenvalue λ_j must be a solution of

$$-\tan\left[d\sqrt{k^2 n^2 - \lambda}\right] \tanh\left[(D - d)\sqrt{\lambda - k^2}\right] = \frac{\sqrt{k^2 n^2 - \lambda}}{\sqrt{\lambda - k^2}}. \tag{3.5}$$

When $kD \to +\infty$, we can approximate the eigenvalues by the solutions in $(k^2, n^2 k^2)$ of the simpler equation

$$-\tan\left[d\sqrt{k^2 n^2 - \lambda}\right] = \frac{\sqrt{k^2 n^2 - \lambda}}{\sqrt{\lambda - k^2}}. \tag{3.6}$$

As proved in appendix A, there are

$$N_s = \left\lceil \frac{kd\sqrt{n^2 - 1}}{\pi} - \frac{1}{2} \right\rceil \tag{3.7}$$

such solutions, where the brackets denote the ceil part, meaning that N_s is the unique integer such that $(N_s - 1/2)\pi < kd\sqrt{n^2 - 1} \leq (N_s + 1/2)\pi$. We assume that $N_s \geq 1$, i.e. $kd\sqrt{n^2 - 1} > \pi/2$.

The eigenfunctions have the form

$$\phi_j(z) = \begin{cases} A_j \sin\left[z\sqrt{k^2 n^2 - \lambda_j}\right], & \text{if } z \in (-d, 0), \\ -A_j \sin\left[d\sqrt{k^2 n^2 - \lambda_j}\right] \exp\left[(d+z)\sqrt{\lambda_j - k^2}\right], & \text{if } z \in (-\infty, -d), \end{cases} \tag{3.8}$$

with A_j defined, up to a sign, by the normalization condition

$$\int_{-\infty}^{0} \phi_j^2(z)\, dz = \frac{A_j^2}{2}\left[d + (\lambda_j^2 - k^2)^{-1/2}\right] = 1. \tag{3.9}$$

Note from equation (3.8) that the eigenfunctions decay exponentially for $z < -d$. As explained in §3c, they define the propagating modes $\phi_j(z)\exp[\pm i\sqrt{\lambda_j}\, x]$ which are trapped near the thin layer, and represent the surface waves in our model.

(b) The eigenfunctions that define the body and evanescent waves

The remaining eigenvalues $(\lambda_j)_{j \geq N_s + 1}$ lie in the spectral interval $(-\infty, k^2)$. The eigenfunctions are of the form

$$\phi_j(z) = \begin{cases} A_j \sin\left[z\sqrt{k^2 n^2 - \lambda_j}\right], & \text{if } z \in (-d, 0), \\ B_j \cos\left[(D+z)\sqrt{k^2 - \lambda_j}\right], & \text{if } z \in (-D, -d), \end{cases} \tag{3.10}$$

with constants A_j and B_j related by

$$B_j = -A_j \frac{\sin\left[d\sqrt{k^2 n^2 - \lambda_j}\right]}{\cos\left[(D-d)\sqrt{k^2 - \lambda_j}\right]}, \tag{3.11}$$

so that (3.10) is continuous at $z = -d$. The normalization condition $\int_{-D}^{0} \phi_j^2(z)dz = 1$ defines A_j up to a sign, and as shown in appendix B, in the regime $kD \gg 1$ we have

$$A_j^2 \simeq \frac{2(k^2 - \lambda_j)}{D\left[k^2 - \lambda_j + k^2(n^2 - 1)\cos^2\left(d\sqrt{k^2 n^2 - \lambda_j}\right)\right]}, \qquad B_j^2 \simeq \frac{2}{D}. \tag{3.12}$$

As in the previous section, the continuity of the derivative of (3.10) gives that the eigenvalues satisfy the equation

$$\tan\left[d\sqrt{k^2 n^2 - \lambda}\right] \tan\left[(D-d)\sqrt{k^2 - \lambda}\right] = \frac{\sqrt{k^2 n^2 - \lambda}}{\sqrt{k^2 - \lambda}}. \tag{3.13}$$

Let N_b denote the number of positive eigenvalues $\lambda_j \in (0, k^2)$. We show in the next section that the corresponding eigenfunctions define the propagating modes $\phi_j(z)\exp[\pm i\sqrt{\lambda_j}x]$ which are large throughout the section of the waveguide, and represent the body waves in our model. The eigenfunctions for the remaining infinitely many eigenvalues[2] lying in the interval $(-\infty, 0)$ define the evanescent modes $\phi_j(z)\exp[-\sqrt{|\lambda_j|}|x|]$.

When D grows, the eigenvalue density increases in $(0, k^2)$, and as proved in appendix B, we have the approximate recursive relation

$$\lambda_j - \lambda_{j+1} \simeq \frac{2\pi}{D}\sqrt{k^2 - \lambda_j}, \quad j = N_s + 1, \ldots, N_s + N_b. \tag{3.14}$$

This leads to the following estimate of the number of body waves

$$N_b \approx \frac{D}{2\pi} \sum_{j=N_s+1}^{N_s+N_b} \frac{\lambda_j - \lambda_{j+1}}{\sqrt{k^2 - \lambda_j}} \approx \frac{D}{2\pi} \int_0^{k^2} \frac{d\lambda}{\sqrt{k^2 - \lambda}} = \frac{kD}{\pi}. \tag{3.15}$$

---

[2]There is a unique sequence of values of D for which $\lambda = 0$ is a solution of (3.13). We assume throughout that even as D grows, it does so outside this set of measure zero.

(c) Mode decomposition in the unperturbed waveguide

We can use the orthonormal $L^2(-D, 0)$ basis of eigenfunctions $(\phi_j(z))_{j\geq 1}$ to write the solution $p_0(x,z)$ of (2.1)–(2.2), with $n_\varepsilon^2(x,z)$ replaced by $n_0^2(z)$, as the following series

$$p_0(x,z) = \sum_{j=1}^{\infty} p_{j,0}(x)\phi_j(z). \tag{3.16}$$

Each term in this series is called a waveguide mode, and $p_{j,0}(x)$ are one-dimensional waves, the solutions of

$$(\partial_x^2 + \lambda_j)p_{j,0}(x) = \delta'(x)\int_{-D}^{0} f(z)\phi_j(z)\,\mathrm{d}z, \quad j \geq 1, \tag{3.17}$$

that are outgoing and bounded at $|x| \to \infty$. There are two types of such waves, depending on the sign of the eigenvalue λ_j. If $\lambda_j > 0$, then $p_{j,0}(x)$ is a propagating wave. Otherwise, it is an evanescent wave.

The expression of the wave field is

$$p_0(x,z) = \begin{cases} \displaystyle\sum_{j=1}^{N} \frac{a_{j,0}}{\sqrt{\beta_j}}\,\mathrm{e}^{\mathrm{i}\beta_j x}\phi_j(z) + \sum_{j \geq N+1} \frac{a_{j,0}}{\sqrt{\beta_j}}\,\mathrm{e}^{-\beta_j x}\phi_j(z), & x > 0, \\[3mm] \displaystyle -\sum_{j=1}^{N} \frac{a_{j,0}}{\sqrt{\beta_j}}\,\mathrm{e}^{-\mathrm{i}\beta_j x}\phi_j(z) - \sum_{j \geq N+1} \frac{a_{j,0}}{\sqrt{\beta_j}}\,\mathrm{e}^{\beta_j x}\phi_j(z), & x < 0, \end{cases} \tag{3.18}$$

where $N = N_\mathrm{s} + N_\mathrm{b}$ is the total number of propagating modes, and we introduced the notation

$$\beta_j = \sqrt{|\lambda_j|}, \quad j \geq 1. \tag{3.19}$$

As explained in §3a, the first N_s propagating modes are essentially supported in the surface layer, so they model surface waves. The remaining N_b propagating modes are called body waves, because as shown in §3b, their transverse profile occupies the entire cross section of the waveguide.

Since the problem in the unperturbed waveguide is separable, the modes are independent, with constant amplitudes determined by the source

$$a_{j,0} = \frac{\sqrt{\beta_j}}{2}\int_{-D}^{0} f(z)\phi_j(z)\,\mathrm{d}z, \quad j \geq 1. \tag{3.20}$$

(d) Mode decomposition in the randomly perturbed waveguide

The solution of (2.1) and (2.2), with the random coefficient $n_\varepsilon^2(x,z)$ defined in (2.3), can also be expanded in the orthonormal eigenbasis

$$p(x,z) = \sum_{j=1}^{\infty} p_j(x)\phi_j(z), \tag{3.21}$$

but the modes are no longer independent due to scattering in the random medium. Instead, the one-dimensional waves $p_j(x)$, for $j \geq 1$, solve the infinite system of coupled ordinary differential equations

$$(\partial_x^2 + \lambda_j)p_j(x) = \delta'(x)\int_{-D}^{0} f(z)\phi_j(z)\,\mathrm{d}z - k^2\varepsilon 1_{(0,L_\varepsilon)}(x)\sum_{l=1}^{\infty} \mu_{jl}(x)p_l(x), \tag{3.22}$$

driven over the range interval $(0, L_\varepsilon)$ by the random, stationary, mean zero processes

$$\mu_{jl}(x) = \int_{-d}^{0} \phi_j(z)\phi_l(z)\nu(x,z)\,\mathrm{d}z, \quad j, l \geq 1. \tag{3.23}$$

Here $1_{(0,L_\varepsilon)}(x)$ is the indicator function equal to 1 for $x \in (0, L_\varepsilon)$ and 0 otherwise.

The propagating waves $p_j(x)$, indexed by $j = 1, \ldots, N$, have both forward and backward going components. At $x < 0$ they satisfy the same equation and radiation condition as in the unperturbed medium, so we can write directly their expression

$$p_j(x) = \frac{b_j^-}{\sqrt{\beta_j}} \, e^{-i\beta_j x}, \quad x < 0, \, j = 1, \ldots, N, \tag{3.24}$$

with constant b_j^- to be determined. For $x > 0$ we use the method of variation of parameters for second-order ordinary differential equations. We introduce the complex-valued amplitudes of the forward and backward going waves $a_j(x)$ and $b_j(x)$ defined by

$$a_j(x) = \frac{1}{2} \left(\sqrt{\beta_j} \, p_j(x) + \frac{1}{i\sqrt{\beta_j}} \partial_x p_j(x) \right) e^{-i\beta_j x},$$

$$b_j(x) = \frac{1}{2} \left(\sqrt{\beta_j} \, p_j(x) - \frac{1}{i\sqrt{\beta_j}} \partial_x p_j(x) \right) e^{i\beta_j x}, \quad j = 1, \ldots, N. \tag{3.25}$$

They satisfy the relation

$$\partial_x a_j(x) \, e^{i\beta_j x} + \partial_x b_j(x) \, e^{-i\beta_j x} = 0, \quad j = 1, \ldots, N, \tag{3.26}$$

so that

$$p_j(x) = \frac{1}{\sqrt{\beta_j}} \left(a_j(x) \, e^{i\beta_j x} + b_j(x) \, e^{-i\beta_j x} \right),$$

$$\partial_x p_j(x) = i\sqrt{\beta_j} \left(a_j(x) \, e^{i\beta_j x} - b_j(x) \, e^{-i\beta_j x} \right), \quad j = 1, \ldots, N. \tag{3.27}$$

Using the jump conditions at $x = 0$, where the source lies,

$$p_j(0^+) - p_j(0^-) = \int_{-D}^0 f(z)\phi_j(z) \, dz, \quad \partial_x p_j(0^+) = \partial_x p_j(0^-), \tag{3.28}$$

we obtain that[3]

$$a_j(0^+) = a_{j,0} = \frac{\sqrt{\beta_j}}{2} \int_{-D}^0 f(z)\phi_j(z) \, dz, \quad b_j^- = b_j(0^+) - a_{j,0}, \tag{3.29}$$

while the radiation condition at $x \to \infty$ gives

$$b_j(x) = 0, \quad x \geq L_\varepsilon, \, j = 1, \ldots, N. \tag{3.30}$$

The cumulative scattering effect of the random medium on the propagating wave is now modelled by the random amplitudes $a_j(x)$ and $b_j(x)$, for $j = 1, \ldots, N$. Their evolution is described by the following system of first-order ordinary differential equations, obtained by substituting equation (3.27) into (3.22) and using (3.26)

$$\partial_x a_j(x) = \frac{ik^2\varepsilon}{2} \sum_{l=1}^N \frac{\mu_{jl}(x)}{\sqrt{\beta_l\beta_j}} \left[a_l(x) \, e^{i(\beta_l - \beta_j)x} + b_l(x) \, e^{-i(\beta_l + \beta_j)x} \right] + \frac{ik^2\varepsilon}{2} \sum_{l \geq N+1} \frac{\mu_{jl}(x)}{\sqrt{\beta_j}} p_l(x) \, e^{-i\beta_j x}, \tag{3.31}$$

and

$$\partial_x b_j(x) = -\frac{ik^2\varepsilon}{2} \sum_{l=1}^N \frac{\mu_{jl}(x)}{\sqrt{\beta_l\beta_j}} \left[a_l(x) \, e^{i(\beta_l + \beta_j)x} + b_l(x) \, e^{-i(\beta_l - \beta_j)x} \right] - \frac{ik^2\varepsilon}{2} \sum_{l \geq N+1} \frac{\mu_{jl}(x)}{\sqrt{\beta_j}} p_l(x) \, e^{i\beta_j x}, \tag{3.32}$$

for $x \in (0, L_\varepsilon)$, with initial condition (3.29) and end condition (3.30). This system of $2N$ equations is coupled with the second-order equations (3.22) for the evanescent waves $p_l(x)$, indexed by $l \geq N + 1$.

---

[3]Because we assume a smooth covariance $\mathcal{C}$ of the random fluctuations, we will see in §4a that the back reflection from the random medium, captured by $b_j(0)$, is negligible when $\varepsilon \to 0$. Therefore, equation (3.24) gives that at $z < 0$ the wave is approximately the same as in the unperturbed waveguide.

4. Effective dynamics for the mode amplitudes

Let us rename the complex mode amplitudes in the large-range scaling as

$$a_j^\varepsilon(x) = a_j\left(\frac{x}{\varepsilon^2}\right), \quad b_j^\varepsilon(x) = b_j\left(\frac{x}{\varepsilon^2}\right), \, j = 1, \ldots, N. \tag{4.1}$$

We are interested in their behaviour in the limit $\varepsilon \to 0$. The stochastic asymptotic analysis is quite involved, but it follows exactly the lines of the analysis in [34,35] and [33, ch. 20]. Therefore, we do not repeat it here and just give in §4a a brief summary and the relevant results for this paper. The radiative transfer equation for the propagating mean mode powers is derived from these results in §4b.

(a) The stochastic limit $\varepsilon \to 0$

The first step in carrying out the limit is to express the evanescent waves $(p_l(x/\varepsilon^2))_{l \geq N+1}$ in terms of the propagating mode amplitudes, so that we obtain a closed system of $2N$ ordinary differential equations for $(a_j^\varepsilon(x), b_j^\varepsilon(x))_{j=1}^N$. This can be done by inverting the operator $\partial_x^2 + \lambda_j$ in (3.22), for $\lambda_j < 0$, using Green's function $G_j(x, x') = [1/(2\beta_j)] e^{-\beta_j|x-x'|}$. This satisfies

$$(\partial_x^2 - \beta_j^2)G_j(x, x') = -\delta(x - x'),$$

and the radiation condition $G_j(x, x') \to 0$ as $|x - x'| \to \infty$. Green's identity transforms (3.22) into an integral equation with ε perturbed term, which can be solved using Neumann series as shown in ([34], Section 3.3) and ([33], Section 20.2). The result is

$$p_j\left(\frac{x}{\varepsilon^2}\right) = \frac{\varepsilon k^2}{2\beta_j} \int_0^{L/\varepsilon^2} e^{-\beta_j\left|\frac{x}{\varepsilon^2} - x'\right|} \sum_{l=1}^N \frac{\mu_{jl}(x')}{\sqrt{\beta_l}} \left[a_l^\varepsilon(x) e^{i\beta_l x'} + b_l^\varepsilon(x) e^{-i\beta_l x'}\right] dx' + O(\varepsilon^2),$$

for $x > 0$ and $j \geq N + 1$. Substituting into (3.31) and (3.32) we obtain a closed system of equations for the propagating mode amplitudes.

The assumed smoothness in x of the covariance function (2.4) and therefore the fast decay of its x-Fourier transform, the power spectral density $\widehat{\mathcal{C}}(\kappa, z, z')$, implies that in the limit $\varepsilon \to 0$ the coupling between the forward-going amplitudes $(a_j^\varepsilon(x))_{j=1}^N$ and the backward-going amplitudes $(b_j^\varepsilon(x))_{j=1}^N$ is negligible ([35], Section 3.3). Due to the homogeneous end condition (3.30), we then conclude that

$$b_j^\varepsilon(x) \approx 0, \quad j = 1, \ldots, N, \, x > 0.$$

This is the forward-scattering approximation and the problem reduces to solving an initial value problem for the system of N equations for $(a_j^\varepsilon(x))_{j=1}^N$, starting from the values (3.29) at $x = 0$. We can finally apply a diffusion-approximation theorem ([33], ch. 6) to this system and obtain the following result.

Theorem 4.1. *As $\varepsilon \to 0$, the $\mathbb{C}^N$-valued random process $(a_j^\varepsilon(x))_{j=1}^N$ converges in distribution in $C^0([0, L], \mathbb{C}^N)$, the space of continuous functions from $[0, L]$ to $\mathbb{C}^N$, to the Markov process $(\mathfrak{a}_j(x))_{j=1}^N$ with infinitesimal generator $\mathcal{L}$. This generator has the form $\mathcal{L} = \mathcal{L}^{(1)} + \mathcal{L}^{(2)}$, where $\mathcal{L}^{(1)}$ and $\mathcal{L}^{(2)}$ are the differential operators:*

$$\mathcal{L}^{(1)} = \frac{1}{2}\sum_{j,l=1}^N (1 - \delta_{jl})\Gamma_{jl}^c\left(\mathfrak{a}_j\overline{\mathfrak{a}_j}\partial_{\mathfrak{a}_l}\partial_{\overline{\mathfrak{a}_l}} + \mathfrak{a}_l\overline{\mathfrak{a}_l}\partial_{\mathfrak{a}_j}\partial_{\overline{\mathfrak{a}_j}} - \mathfrak{a}_j\mathfrak{a}_l\partial_{\mathfrak{a}_j}\partial_{\mathfrak{a}_l} - \overline{\mathfrak{a}_j\mathfrak{a}_l}\partial_{\overline{\mathfrak{a}_j}}\partial_{\overline{\mathfrak{a}_l}}\right)$$

$$+ \frac{1}{2}\sum_{j,l=1}^N \Gamma_{jl}^p\left(\mathfrak{a}_j\overline{\mathfrak{a}_l}\partial_{\mathfrak{a}_j}\partial_{\overline{\mathfrak{a}_l}} + \overline{\mathfrak{a}_j}\mathfrak{a}_l\partial_{\overline{\mathfrak{a}_j}}\partial_{\mathfrak{a}_l} - \mathfrak{a}_j\mathfrak{a}_l\partial_{\mathfrak{a}_j}\partial_{\mathfrak{a}_l} - \overline{\mathfrak{a}_j\mathfrak{a}_l}\partial_{\overline{\mathfrak{a}_j}}\partial_{\overline{\mathfrak{a}_l}}\right)$$

$$+ \frac{1}{2}\sum_{j=1}^N (\Gamma_{jj}^c - \Gamma_{jj}^p)(\mathfrak{a}_j\partial_{\mathfrak{a}_j} + \overline{\mathfrak{a}_j}\partial_{\overline{\mathfrak{a}_j}}) + \frac{i}{2}\sum_{j=1}^N \Gamma_{jj}^s(\mathfrak{a}_j\partial_{\mathfrak{a}_j} - \overline{\mathfrak{a}_j}\partial_{\overline{\mathfrak{a}_j}}) \tag{4.2}$$

and

$$\mathcal{L}^{(2)} = i \sum_{j=1}^{N} \kappa_j \left(\mathfrak{a}_j \partial_{\mathfrak{a}_j} - \overline{\mathfrak{a}_j} \partial_{\overline{\mathfrak{a}_j}} \right). \tag{4.3}$$

Here we use the classical complex derivative: if $\zeta = \zeta_r + i\zeta_i$, *then* $\partial_\zeta = (1/2)(\partial_{\zeta_r} - i\partial_{\zeta_i})$ *and* $\partial_{\overline{\zeta}} = (1/2)(\partial_{\zeta_r} + i\partial_{\zeta_i})$. *The coefficients in (4.2) and (4.3) are defined as follows:*

— *For all* $j, l = 1, \dots, N$, *with* $j \neq l$, Γ_{jl}^c *and* Γ_{jl}^s *are given by*

$$\Gamma_{jl}^c = \frac{k^4}{2\beta_j\beta_l} \int_0^\infty C_{jl}(x) \cos\left[(\beta_l - \beta_j)x\right] dx, \quad \text{and} \quad \Gamma_{jl}^s = \frac{k^4}{2\beta_j\beta_l} \int_0^\infty C_{jl}(x) \sin\left[(\beta_l - \beta_j)x\right] dx, \tag{4.4}$$

with $C_{jl}(x)$ *defined by*

$$C_{jl}(x) = \mathbb{E}[\mu_{jl}(0)\mu_{jl}(x)], \tag{4.5}$$

where[4]

$$\mathbb{E}[\mu_{jl}(0)\mu_{j'l'}(x)] \overset{(3.23)}{=} \int_{-d}^0 \int_{-d}^0 \phi_j(z)\phi_l(z)C(x, z, z')\phi_{j'}(z')\phi_{l'}(z')\, dz dz'. \tag{4.6}$$

— *For all* $j, l = 1, \dots, N$:

$$\Gamma_{jl}^p = \frac{k^4}{4\beta_j\beta_l} \int_0^\infty \left\{ \mathbb{E}[\mu_{jj}(0)\mu_{ll}(x)] + \mathbb{E}[\mu_{ll}(0)\mu_{jj}(x)] \right\} dx. \tag{4.7}$$

— *For all* $j = 1, \dots, N$:

$$\Gamma_{jj}^c = -\sum_{l=1, l\neq j}^{N} \Gamma_{jl}^c, \quad \Gamma_{jj}^s = -\sum_{l=1, l\neq j}^{N} \Gamma_{jl}^s, \quad \kappa_j = \sum_{l=N+1}^{\infty} \frac{k^4}{2\beta_l\beta_j} \int_0^\infty C_{jl}(x) \cos(\beta_j x) e^{-\beta_l x}\, dx. \tag{4.8}$$

We remark that the operator $\mathcal{L}^{(1)}$ models the effect of the coupling between the propagating modes, and we show in the next section that it determines the power exchange between these modes. The operator $\mathcal{L}^{(2)}$ is due to the coupling with the evanescent modes and gives rise to additional phase terms (effective dispersion) of the limit amplitudes of the propagating modes. However, it has no effect on the transfer of power among these modes.

One can verify by direct calculation that

$$\mathcal{L}\left(\sum_{j=1}^{N} |\mathfrak{a}_j|^2 \right) = 0, \tag{4.9}$$

so the process $(\mathfrak{a}_j(x))_{j=1}^N$ is supported on the sphere of $\mathbb{C}^N$ centred at 0 and with radius R, where

$$R^2 = \sum_{l=1}^{N} |a_{l,0}|^2. \tag{4.10}$$

The operator $\mathcal{L}$ is not self-adjoint on this sphere, due to the terms Γ_{jj}^s and κ_j, so the process is not reversible. However, the uniform measure on the sphere is invariant and $\mathcal{L}$ is strongly elliptic. This implies that $(\mathfrak{a}_j(x))_{j=1}^N$ is an ergodic process and its distribution converges as $x \to \infty$ to the uniform distribution over the sphere.

Note that theorem 4.1 uses the forward scattering approximation. If backscattering is significant, then our analysis cannot be readily extended, because we lose the Markov property that is instrumental in the proof of the diffusion-approximation theorem.

---

[4]Note that the integrals in (4.6) are computed on the domain $z \in (-d, 0)$ where the random medium lies, and not the entire cross section of the waveguide.

(b) The radiative transfer equation

Denote the limit mode powers by

$$\mathfrak{P}_j(x) = |\mathfrak{a}_j(x)|^2, \quad j = 1, \ldots, N. \tag{4.11}$$

If the generator $\mathcal{L}$ described in theorem 4.1 is applied to a test function that depends only on these mode powers, then the result is a function that depends only on the mode powers, as well. This leads to the following corollary:

Corollary 4.2. *The process* $(|a_j^\varepsilon(x)|^2)_{j=1}^N$ *converges in the limit* $\varepsilon \to 0$ *to a Markov process* $(\mathfrak{P}_j(x))_{j=1}^N$ *whose infinitesimal generator* $\mathcal{L}_\mathfrak{P}$ *is given by*

$$\mathcal{L}_\mathfrak{P} = \sum_{j,l=1, j \neq l}^N \Gamma_{jl}^c \big[\mathfrak{P}_l \mathfrak{P}_j (\partial_{\mathfrak{P}_j} - \partial_{\mathfrak{P}_l}) \partial_{\mathfrak{P}_j} + (\mathfrak{P}_l - \mathfrak{P}_j) \partial_{\mathfrak{P}_j} \big], \tag{4.12}$$

with Γ_{jl}^c *defined in (4.4).*

It is easy to conclude from the form of the generator (4.12) that the nth-order moments of the mode powers satisfy closed equations. We are particularly interested in the mean mode powers

$$P_j(x) = \mathbb{E}[\mathfrak{P}_j(x)], \tag{4.13}$$

and obtain, using corollary 4.2, that they satisfy the following system of radiative transfer equations

$$\partial_x P_j(x) = \sum_{l=1}^N \Gamma_{jl}^c [P_l(x) - P_j(x)], \quad x > 0, \quad P_j(0) = |a_{j,0}|^2, \, j = 1, \ldots, N. \tag{4.14}$$

These equations can be solved explicitly using the exponential of the matrix $\boldsymbol{\Gamma}^c = (\Gamma_{j,l}^c)_{j,l=1}^N$

$$\boldsymbol{P}(x) = \exp(\boldsymbol{\Gamma}^c x) \boldsymbol{P}(0), \quad \boldsymbol{P}(x) = (P_1(x), \ldots, P_N(x))^\mathsf{T}. \tag{4.15}$$

We can estimate the initial cumulative (total) power of the propagating modes $\|\boldsymbol{P}(0)\|_1 = R^2$ using equations (4.10), (3.20) and (3.19), as follows

$$\|\boldsymbol{P}(0)\|_1 = \sum_{j=1}^N \frac{\lambda_j}{4} \left| \int_{-D}^0 f(z) \phi_j(z) \, dz \right|^2 < \frac{n^2 k^2}{4} \sum_{j=1}^N \left| \int_{-D}^0 f(z) \phi_j(z) \, dz \right|^2 < \frac{n^2 k^2}{4} \|f\|_{L^2}^2. \tag{4.16}$$

Here the first inequality is because $\lambda_j \in (0, n^2 k^2)$ for $j = 1, \ldots, N$ and the second inequality is by Parseval's identity for the expansion in the orthonormal eigenbasis $(\phi_j(z))_{j \geq 1}$. Thus, the total power is uniformly bounded with respect to D and therefore N_b, when f is square integrable.

In the next section, we use equation (4.15) to analyse the transfer of power between the surface and the body waves and the transition to equipartition.

5. Convergence to equipartition

Equation (4.15) shows that the evolution of the mean mode powers is dictated by the matrix $\boldsymbol{\Gamma}^c$ with off-diagonal entries (4.4) and diagonal entries (4.8). Note that the off-diagonal entries are non-negative, because they are power spectral densities of stationary random processes, and that the rows sum to 0. Therefore, 0 is an eigenvalue, for the un-normalized eigenvector $\boldsymbol{1}_N$ with all entries equal to 1.

We assume henceforth that $\boldsymbol{\Gamma}^c$ is an irreducible matrix. This is a very weak assumption and it means that there are not too many zeros in $\boldsymbol{\Gamma}^c$, which is typical for the covariance functions used in our analysis. More precisely, the assumption is that for any pair $j \neq l$, there exists m and a sequence $j_0, \ldots, j_m$ with $j_0 = j$ and $j_m = l$, so that $\Gamma_{j_p, j_{p+1}}^c > 0$ for all $p = 0, \ldots, m - 1$. We can then conclude from the Perron–Frobenius theorem that 0 is the largest eigenvalue, which is simple. This implies that the mean mode power vector (4.15) converges to a vector that is a multiple of

1_N as $x \to \infty$. That is to say, the system reaches equipartition, where the power is distributed uniformly over the modes. The range at which equipartition is reached is the reciprocal of the absolute value of the largest non-zero eigenvalue of $\boldsymbol{\Gamma}^c$ ([33], ch. 20).

In this section, we study how the surface and body waves interact during the transition to equipartition, by taking a second limit $kD \to \infty$. Recall that the width d of the surface layer is fixed and of the order of the wavelength, so the number N_s of surface wave modes converges to the positive and finite limit (3.7). Recall also from equation (3.15) that the number $N_b = N - N_s$ of body waves is proportional to kD. Therefore, taking $kD \to \infty$ is equivalent to letting $N_b \to \infty$.

To carry out the analysis, we sort the entries in $\boldsymbol{\Gamma}^c$ based on how they depend on N_b. We see from equations (3.8) and (3.9) that the first N_s mode profiles have a finite limit as $kD \to \infty$. Therefore, the block $(\Gamma^c_{j,l})^{N_s}_{j,l=1}$ has $O(1)$ entries. The body wave profiles are supported in $(-D, 0)$ and have amplitudes of order $\sqrt{2/D} = O(\sqrt{k/N_b})$, by (3.10)–(3.12). Using these estimates in definition (4.4) we get that $\boldsymbol{\Gamma}^c$ has the following block structure

$$\boldsymbol{\Gamma}^c = \begin{pmatrix} \boldsymbol{\Gamma}^{(0)} - \boldsymbol{\Lambda} & \dfrac{1}{N_b}\boldsymbol{\Gamma}^{(1)} \\[2ex] \dfrac{1}{N_b}\boldsymbol{\Gamma}^{(1)\mathrm{T}} & \dfrac{1}{N_b^2}\boldsymbol{\Gamma}^{(2)} - \dfrac{1}{N_b}\widetilde{\boldsymbol{\Lambda}} \end{pmatrix} \tag{5.1}$$

where the blocks $\boldsymbol{\Gamma}^{(0)}$, $\boldsymbol{\Gamma}^{(1)}$, $\boldsymbol{\Lambda}$ and $\widetilde{\boldsymbol{\Lambda}}$ have $O(1)$ entries, while the block $\boldsymbol{\Gamma}^{(2)}$ has $O(1)$ off-diagonal entries.

The entries in the off-diagonal block $\boldsymbol{\Gamma}^{(1)} \in \mathbb{R}^{N_s \times N_b}$ are just the scaled version of those in $\boldsymbol{\Gamma}^c$,

$$\Gamma^{(1)}_{jl} = N_b \Gamma^c_{j(l+N_s)}, \quad j = 1, \ldots, N_s, \; l = 1, \ldots, N_b. \tag{5.2}$$

The first diagonal block in (5.1) is the difference of two $N_s \times N_s$ matrices: The first one is $\boldsymbol{\Gamma}^{(0)}$ with entries

$$\Gamma^{(0)}_{jl} = \Gamma^c_{jl}, \quad 1 \le j, l \le N_s, \; j \ne l, \quad \Gamma^{(0)}_{jj} = -\sum_{l=1,l\ne j}^{N_s} \Gamma^{(0)}_{jl}, \; 1 \le j \le N_s, \tag{5.3}$$

whose rows are summing to zero. The second matrix $\boldsymbol{\Lambda}$ is diagonal, with positive entries

$$\Lambda_{jj} = \frac{1}{N_b} \sum_{l=1}^{N_b} \Gamma^{(1)}_{jl}, \quad 1 \le j \le N_s. \tag{5.4}$$

The second diagonal block in (5.1) is the difference of two $N_b \times N_b$ matrices: The first one is defined by $\boldsymbol{\Gamma}^{(2)}$ with off-diagonal entries $\Gamma^{(2)}_{jl}$ and rows summing to zero,

$$\Gamma^{(2)}_{jj} = -\sum_{l=1,l\ne j}^{N_s} \Gamma^{(2)}_{jl}, \quad 1 \le j \le N_b, \tag{5.5}$$

and the second one is defined by the diagonal matrix $\widetilde{\boldsymbol{\Lambda}}$ with non-negative entries

$$\widetilde{\Lambda}_{jj} = \sum_{l=1}^{N_s} \Gamma^{(1)}_{lj}, \quad 1 \le j \le N_b. \tag{5.6}$$

Note that both diagonal blocks of $\boldsymbol{\Gamma}^c$ are negative definite, symmetric matrices.

In the next two sections, we use this block structure of $\boldsymbol{\Gamma}^c$ to carry out the analysis of convergence to equipartition. We begin in §5a with a simplified model which allows a quick and explicit convergence analysis that gives some insight into how the surface and body waves interact. Then we consider the general model in §5b and we discuss the results in §5c.

(a) Simplified model

Consider the particular case where the entries in the blocks $\boldsymbol{\Gamma}^{(1)}$ and $\boldsymbol{\Gamma}^{(2)}$ satisfy

$$\Gamma_{jl}^{(1)} = \gamma_1, \quad 1 \leq j \leq N_s, \ 1 \leq l \leq N_b, \tag{5.7}$$

and

$$\Gamma_{jl}^{(2)} = \gamma_2, \quad 1 \leq j, l \leq N_b, \ j \neq l, \tag{5.8}$$

for some positive constants γ_1 and γ_2. Then, the diagonal matrices (5.4) and (5.6) are multiples of the identity matrices $\mathbf{I}_{N_s} \in \mathbb{R}^{N_s \times N_s}$ and $\mathbf{I}_{N_b} \in \mathbb{R}^{N_b \times N_b}$:

$$\boldsymbol{\Lambda} = \gamma_1 \mathbf{I}_{N_s}, \quad \widetilde{\boldsymbol{\Lambda}} = N_s \gamma_1 \mathbf{I}_{N_b}, \tag{5.9}$$

and we can obtain an explicit spectral decomposition of $\boldsymbol{\Gamma}^c$, for any N_b (large or not):

Let us denote by $-g_1, \ldots, -g_{N_s}$ the eigenvalues of $\boldsymbol{\Gamma}^{(0)}$ sorted in decreasing order. Note that $v_1 = (1/\sqrt{N_s})\mathbf{1}_{N_s}$ is an eigenvector of $\boldsymbol{\Gamma}^{(0)}$, for the eigenvalue 0, where we recall that $\mathbf{1}_{N_s}$ is the vector in $\mathbb{R}^{N_s}$ with all entries equal to 1. In fact, by the Perron–Frobenius theorem, $-g_1 = 0$ is the leading eigenvalue and it is simple. Since $\boldsymbol{\Gamma}^{(0)}$ is symmetric, it can be diagonalized

$$\boldsymbol{\Gamma}^{(0)} = \mathbf{V}\,\mathrm{Diag}\big(0, -g_2, \ldots, -g_{N_s}\big)\mathbf{V}^{\mathsf{T}}, \tag{5.10}$$

where $\mathbf{V}$ is the orthogonal matrix of the eigenvectors $(v_j)_{j=1}^{N_s}$. Similarly, we can diagonalize $\boldsymbol{\Gamma}^{(2)}$

$$\boldsymbol{\Gamma}^{(2)} = \gamma_2 \mathbf{1}_{N_b}\mathbf{1}_{N_b}^{\mathsf{T}} - \gamma_2 N_b \mathbf{I}_{N_b} = \mathbf{W}\,\mathrm{Diag}\big(0, -\gamma_2 N_b, \ldots, -\gamma_2 N_b\big)\mathbf{W}^{\mathsf{T}}, \tag{5.11}$$

where $\mathbf{W} = (w_j)_{j=1}^{N_b}$ is an orthogonal matrix with first column $w_1 = \frac{1}{\sqrt{N_b}}\mathbf{1}_{N_b}$.

Using these spectral decompositions and the relations

$$\boldsymbol{\Gamma}^{(1)}w_j = \sqrt{N_s N_b}\, v_1 \delta_{j1}, \quad 1 \leq j \leq N_b, \quad \boldsymbol{\Gamma}^{(1)^{\mathsf{T}}}v_j = \sqrt{N_s N_b}\, w_1 \delta_{j1}, \ 1 \leq j \leq N_s, \tag{5.12}$$

we obtain that $\boldsymbol{\Gamma}^c$ has the following eigenvalues (sorted in decreasing order) and orthonormal eigenvectors:

— The first eigenvalue is simple and equal to 0, for the eigenvector $(1/\sqrt{N})\mathbf{1}_N$, as expected from the Perron–Frobenius theorem.
— The next eigenvalue is equal to $-(\gamma_2 + \gamma_1 N_s)/N_b$, and approaches 0 as $N_b \to \infty$. This eigenvalue has multiplicity $N_b - 1$ and the corresponding eigenvectors are $(\mathbf{0}^{\mathsf{T}}, w_j^{\mathsf{T}})^{\mathsf{T}}$, for $j = 2, \ldots, N_b$.
— The next eigenvalue is equal to $-\gamma_1(1 + N_s/N_b)$. It is simple, and has the finite limit $-\gamma_1$ as $N_b \to \infty$. The eigenvector is $(\sqrt{N_b/N}v_1^{\mathsf{T}}, -\sqrt{N_s/N}w_1^{\mathsf{T}})^{\mathsf{T}}$.
— The remaining $N_s - 1$ eigenvalues $-(g_j + \gamma_1)$ are the eigenvalues of $\boldsymbol{\Gamma}^{(0)}$ shifted by $-\gamma_1$. The eigenvectors are $(v_j^{\mathsf{T}}, \mathbf{0}^{\mathsf{T}})^{\mathsf{T}}$, for $j = 2, \ldots, N_s$.

Let us organize the surface wave powers in the vector $S(x) = (P_1(x), \ldots, P_{N_s}(x))^{\mathsf{T}}$ and the body wave powers in the vector $B(x) = (P_{N_s+1}(x), \ldots, P_N(x))^{\mathsf{T}}$. With the explicit spectral decomposition of $\boldsymbol{\Gamma}^c$ given above, we can now calculate the matrix exponential in (4.15) and obtain that the mean powers of the surface waves are

$$S(x) = \frac{R_{s,0}^2}{N}\left\{1 + \frac{N_b}{N_s}\exp\left[-\gamma_1\left(1 + \frac{N_s}{N_b}\right)x\right]\right\}\mathbf{1}_{N_s} + \frac{R_{b,0}^2}{N}\left\{1 - \exp\left[-\gamma_1\left(1 + \frac{N_s}{N_b}\right)x\right]\right\}\mathbf{1}_{N_s}$$

$$+ \sum_{j=2}^{N_s}\exp\big[-(g_j + \gamma_1)x\big](v_j^{\mathsf{T}}S_0)v_j, \tag{5.13}$$

and the mean powers of the body waves are

$$B(x) = \frac{R_{s,0}^2}{N}\left\{1 - \exp\left[-\gamma_1\left(1 + \frac{N_s}{N_b}\right)x\right]\right\}\mathbf{1}_{N_b} + \frac{R_{b,0}^2}{N}\left\{1 + \frac{N_s}{N_b}\exp\left[-\gamma_1\left(1 + \frac{N_s}{N_b}\right)x\right]\right\}\mathbf{1}_{N_b}$$

$$+ \exp\left[-\frac{(\gamma_2 + \gamma_1 N_s)}{N_b}x\right]\left(B_0 - \frac{R_{b,0}^2}{N_b}\mathbf{1}_{N_b}\right). \tag{5.14}$$

Here we let

$$S_0 = S(0) = \left(|a_{1,0}|^2, \ldots, |a_{N_s,0}|^2\right)^{\mathrm{T}} \quad \text{and} \quad B_0 = B(0) = \left(|a_{N_s+1,0}|^2, \ldots, |a_{N,0}|^2\right)^{\mathrm{T}}$$

be the vectors of initial powers, determined by the source excitation, and we introduced the initial cumulative powers of the surface and body waves

$$R_{s,0}^2 = \sum_{j=1}^{N_s} P_j(0), \quad R_{b,0}^2 = \sum_{j=N_s+1}^{N} P_j(0). \tag{5.15}$$

Observe that summing in equations (5.13)–(5.14) we get

$$\sum_{j=1}^{N} P_j(x) = R_{s,0}^2 + R_{b,0}^2 = R^2. \tag{5.16}$$

This is the conservation of energy described in §4a and equations (4.9)–(4.10).

The fastest decay in equation (5.13) is exhibited by the terms in the last sum. For range $x > (g_2 + \gamma_1)^{-1}$, this sum becomes negligible and the mean surface wave powers become equipartitioned. However, even though the power is uniformly distributed among these waves, their cumulative power still evolves

$$R_s^2(x) = \sum_{j=1}^{N_s} P_j(x)$$

$$= \frac{R^2 N_s}{N} + \frac{(R_{s,0}^2 N_b - R_{b,0}^2 N_s)}{N}\exp\left[-\gamma_1\left(1 + \frac{N_s}{N_b}\right)x\right], \tag{5.17}$$

on the length scale $[\gamma_1(1 + N_s/N_b)]^{-1} \approx \gamma_1^{-1}$. This is due to the slow dynamics of the power exchange with the body waves.

The last term in equation (5.14) shows that the body waves relaxation to equipartition happens on the very large length scale $N_b/(\gamma_2 + N_s\gamma_1)$. After this distance, the exponentials in the first two terms of (5.14) are essentially zero and the body waves are in equipartition, with net power $R_b^2(x) = \sum_{j=N_s+1}^{N} P_j(x)$ equal to $R^2 N_b/N$. The net power of the surface waves tends to the constant $R^2 N_s/N$ by (5.17).

In summary, this simple model reveals that while approaching the equipartition regime, the surface and body wave power exchange occurs as follows:

— First, the surface waves undergo a rapid relaxation towards equipartition amongst themselves, on the range scale $(g_2 + \gamma_1)^{-1}$.
— Then, there is a slower conversion mechanism between the surface waves and the body waves on the range scale γ_1^{-1}.
— The body waves undergo a very slow relaxation towards equipartition, on the range scale $N_b/(\gamma_2 + N_s\gamma_1)$.
— Once the body waves reach equipartition, the whole system is in equipartition.

Note that even if we set $\gamma_2 = 0$, meaning that there is no conversion among the body waves, we still have convergence to equipartition of the body waves by the mechanism 'conversion from body waves to surface waves' followed by 'conversion from surface waves to body waves'.

15

royalsocietypublishing.org/journal/rspa Proc. R. Soc. A 477: 20200775

In general, the comparison between γ_2 and $N_s\gamma_1$ tells us which mechanism is dominant to achieve this equipartition: the first mechanism governs the direct conversion between body waves, while the second one governs the conversion mediated by surface waves. The first mechanism dominates the second one if $\gamma_2 > N_s\gamma_1$.

Note also that the surface waves reach equipartition among themselves as soon as x is larger than the first range scale $(g_2 + \gamma_1)^{-1}$, while the body waves reach equipartition only when x is larger than the third range scale $N_b/(\gamma_2 + N_s\gamma_1)$. As we will see below, the fact that the surface modes reach a metastable equilibrium at the first range scale is a universal feature, but that this metastable equilibrium is a uniform distribution is very special and happens only for the simplified model. In general the metastable equilibrium of the surface modes slowly evolves at the third range scale and eventually becomes uniform when the body waves reach equipartition, as we will see below.

(b) General model

In the general case, it is not possible to get an explicit spectral decomposition of the matrix $\boldsymbol{\Gamma}^c$, but we can obtain estimates of the mean mode powers as we now explain. Let us denote by

$$\boldsymbol{\Gamma} = \boldsymbol{\Gamma}^{(0)} - \boldsymbol{\Lambda}, \quad \widetilde{\boldsymbol{\Gamma}} = \frac{\boldsymbol{\Gamma}^{(2)}}{N_b} - \widetilde{\boldsymbol{\Lambda}}, \tag{5.18}$$

the diagonal blocks in (5.1) and recall that they are symmetric, diagonally dominant and negative definite matrices. The matrix $\boldsymbol{\Gamma}$ has size $N_s \times N_s$ and $O(1)$ entries, $\widetilde{\boldsymbol{\Gamma}}$ has size $N_b \times N_b$, $O(1)$ diagonal entries, and $O(1/N_b)$ off-diagonal entries. The matrix $\boldsymbol{\Gamma}^{(1)}$ that defines the off-diagonal blocks in (5.1) has size $N_s \times N_b$ and $O(1)$ entries.

Integrating the radiative transfer equation (4.14) we obtain that

$$S(x) = \exp(\boldsymbol{\Gamma} x)S_0 + \frac{1}{N_b}\int_0^x \exp(\boldsymbol{\Gamma} x')\boldsymbol{\Gamma}^{(1)}B(x - x')\,\mathrm{d}x' \tag{5.19}$$

and

$$B(x) = \exp\left(\widetilde{\boldsymbol{\Gamma}}\frac{x}{N_b}\right)B_0 + \frac{1}{N_b}\int_0^x \exp\left(\widetilde{\boldsymbol{\Gamma}}\frac{x'}{N_b}\right)\boldsymbol{\Gamma}^{(1)\mathrm{T}}S(x - x')\,\mathrm{d}x', \tag{5.20}$$

where we recall from the previous section that $S(x) \in \mathbb{R}^{N_s}$ and $B(x) \in \mathbb{R}^{N_b}$ are the vectors of mean powers of the surface and body waves and $S_0 = S(0)$ and $B_0 = B(0)$ are the vectors of initial powers determined by the source. We use next these equations to analyse how scattering redistributes the power at $x > 0$.

(i) Mean powers at intermediate range $x \ll N_b$

We show in appendix C that for range $0 < x \ll N_b$, the mean powers of the surface modes are

$$S(x) = \left\{ \exp\left(\boldsymbol{\Gamma} x\right) + \frac{1}{N_b^2}\int_0^x \exp\left(\boldsymbol{\Gamma}(x - x')\right)\boldsymbol{\Gamma}^{-1}\boldsymbol{\Gamma}^{(1)}\boldsymbol{\Gamma}^{(1)\mathrm{T}}\exp\left(\boldsymbol{\Gamma} x'\right)\mathrm{d}x' \right.$$

$$\left. - \frac{1}{N_b^2}\boldsymbol{\Gamma}^{-1}\boldsymbol{\Gamma}^{(1)}\boldsymbol{\Gamma}^{(1)\mathrm{T}}\boldsymbol{\Gamma}^{-1}\left[\exp\left(\boldsymbol{\Gamma} x\right) - \mathbf{I}_{N_s}\right] \right\}S_0$$

$$+ \frac{1}{N_b}\boldsymbol{\Gamma}^{-1}\left[\exp\left(\boldsymbol{\Gamma} x\right) - \mathbf{I}_{N_s}\right]\boldsymbol{\Gamma}^{(1)}B_0 + o\left(\frac{R^2}{N_b}\right). \tag{5.21}$$

Since $\boldsymbol{\Gamma}^{(1)}$ is an $N_s \times N_b$ matrix with $O(1)$ entries, we note that $\boldsymbol{\Gamma}^{(1)}\boldsymbol{\Gamma}^{(1)\mathrm{T}}$ is an $N_s \times N_s$ matrix with $O(N_b)$ entries. The vector $\boldsymbol{\Gamma}^{(1)}B_0$ has $O(R_{b,0}^2)$ entries, which are bounded independent of N_b, as follows from (4.16). Therefore, the terms written explicitly in (5.21) are at least $O(R^2/N_b)$, whereas the residual is $o(R^2/N_b)$.

We also obtain in appendix C the following estimate of the mean powers of the body modes at range $1 \ll x \ll N_b$:

$$B(x) = \exp\left(\tilde{\boldsymbol{\Gamma}} \frac{x}{N_b}\right) B_0 + \frac{1}{N_b} \boldsymbol{\Gamma}^{(1)^\mathrm{T}} \boldsymbol{\Gamma}^{-1} [\exp(\boldsymbol{\Gamma} x) - \mathbf{I}_{N_s}] S_0 + o\left(\frac{R^2}{N_b}\right). \tag{5.22}$$

These expressions reveal the multi-scale nature of the evolution of the mode powers: The surface wave powers evolve quickly, on a range scale $O(1)$, after which the exponentials in (5.21) become negligible and we get the approximate expression (see appendix C):

$$S(x) \approx -\frac{1}{N_b} \boldsymbol{\Gamma}^{-1} \boldsymbol{\Gamma}^{(1)} B_0 + \frac{1}{N_b{}^2} \boldsymbol{\Gamma}^{-1} \boldsymbol{\Gamma}^{(1)} \boldsymbol{\Gamma}^{(1)^\mathrm{T}} \boldsymbol{\Gamma}^{-1} S_0, \quad \text{for } 1 \ll x \ll N_b, \tag{5.23}$$

where the range x dependence is in the lower-order terms. This result is similar to what we saw in the simplified model, but the distribution of power among the surface waves is not uniform, unless the entries in $\boldsymbol{\Gamma}^{(1)}$ are equal to each other, as assumed in §5a. Also similar to the results in §5a, the body wave powers evolve slowly on a range scale of order N_b. At shorter range, they can be approximated by the expression

$$B(x) \approx \exp\left(\tilde{\boldsymbol{\Gamma}} \frac{x}{N_b}\right) B_0 - \frac{1}{N_b} \boldsymbol{\Gamma}^{(1)^\mathrm{T}} \boldsymbol{\Gamma}^{-1} S_0, \quad \text{for } 1 \ll x \ll N_b. \tag{5.24}$$

(ii) Mean powers at range $x = O(N_b)$

It is only at range $x = N_b X$, with $X = O(1)$, that the power transfer among the body waves becomes significant, as seen from the following expression derived in appendix C

$$B(N_b X) \approx \exp\left[\left(\tilde{\boldsymbol{\Gamma}} - \frac{1}{N_b} \boldsymbol{\Gamma}^{(1)^\mathrm{T}} \boldsymbol{\Gamma}^{-1} \boldsymbol{\Gamma}^{(1)}\right) X\right] \left[B_0 - \frac{1}{N_b} \boldsymbol{\Gamma}^{(1)^\mathrm{T}} \boldsymbol{\Gamma}^{-1} S_0\right]. \tag{5.25}$$

Moreover, the body waves interact with the surface waves whose mean powers become

$$S(N_b X) \approx -\frac{1}{N_b} \boldsymbol{\Gamma}^{-1} \boldsymbol{\Gamma}^{(1)} B(N_b X)$$

$$\stackrel{(5.25)}{\approx} -\frac{1}{N_b} \boldsymbol{\Gamma}^{-1} \boldsymbol{\Gamma}^{(1)} \exp\left[\left(\tilde{\boldsymbol{\Gamma}} - \frac{1}{N_b} \boldsymbol{\Gamma}^{(1)^\mathrm{T}} \boldsymbol{\Gamma}^{-1} \boldsymbol{\Gamma}^{(1)}\right) X\right] \left[B_0 - \frac{1}{N_b} \boldsymbol{\Gamma}^{(1)^\mathrm{T}} \boldsymbol{\Gamma}^{-1} S_0\right]. \tag{5.26}$$

(iii) Equipartition

We now use equations (5.25) and (5.26) to show the convergence to equipartition: We prove in appendix D the following identity:

$$\frac{1}{N_b} \boldsymbol{\Gamma}^{-1} \boldsymbol{\Gamma}^{(1)} \mathbf{1}_{N_b} = -\mathbf{1}_{N_s}, \tag{5.27}$$

which in conjunction with (5.26) shows that the surface wave powers are in equipartition, as soon as the body waves $B(N_b X)$ reach equipartition.

It remains to describe the convergence of the body wave powers to equipartition, which is dictated in (5.25) by the exponential of the matrix

$$\tilde{\boldsymbol{\Gamma}} - \frac{1}{N_b} \boldsymbol{\Gamma}^{(1)^\mathrm{T}} \boldsymbol{\Gamma}^{-1} \boldsymbol{\Gamma}^{(1)} \stackrel{(5.18)}{=} \frac{1}{N_b} \boldsymbol{\Gamma}^{(2)} - \tilde{\boldsymbol{\Lambda}} - \frac{1}{N_b} \boldsymbol{\Gamma}^{(1)^\mathrm{T}} \boldsymbol{\Gamma}^{-1} \boldsymbol{\Gamma}^{(1)}. \tag{5.28}$$

The first term in the right-hand side is a symmetric, negative semi-definite matrix with null space span$\{\mathbf{1}_{N_b}\}$, and the last term is a positive definite matrix, because $\boldsymbol{\Gamma}$ and thus $\boldsymbol{\Gamma}^{-1}$ are negative definite. The matrix in (5.28) is N_b times the Schur complement of the block $\boldsymbol{\Gamma} = \boldsymbol{\Gamma}^{(0)} - \boldsymbol{\Lambda}$ in the matrix $\boldsymbol{\Gamma}^{(c)}$ in (5.1). By our assumption on $\boldsymbol{\Gamma}^c$, the matrix in (5.28) is non-negative definite and irreducible, so we can conclude from the Perron–Frobenius theorem that it has a simple leading eigenvalue, with an eigenvector that has positive entries. The remaining eigenvectors have entries

with changing signs, due to orthogonality. We can verify using the identity

$$\frac{1}{N_b}\boldsymbol{\Gamma}^{(1)\mathrm{T}}\boldsymbol{\Gamma}^{-1}\boldsymbol{\Gamma}^{(1)}\mathbf{1}_{N_b} = -\tilde{\boldsymbol{\Lambda}}\mathbf{1}_{N_b}, \tag{5.29}$$

proved in appendix D, that

$$\left[\tilde{\boldsymbol{\Gamma}} - \frac{1}{N_b}\boldsymbol{\Gamma}^{(1)\mathrm{T}}\boldsymbol{\Gamma}^{-1}\boldsymbol{\Gamma}^{(1)}\right]\mathbf{1}_{N_b} \stackrel{(5.28)}{=} \frac{1}{N_b}\boldsymbol{\Gamma}^{(2)}\mathbf{1}_{N_b} - \tilde{\boldsymbol{\Lambda}}\mathbf{1}_{N_b} - \frac{1}{N_b}\boldsymbol{\Gamma}^{(1)\mathrm{T}}\boldsymbol{\Gamma}^{-1}\boldsymbol{\Gamma}^{(1)}\mathbf{1}_{N_b}$$

$$\stackrel{(5.29)}{=} \frac{1}{N_b}\boldsymbol{\Gamma}^{(2)}\mathbf{1}_{N_b} - \tilde{\boldsymbol{\Lambda}}\mathbf{1}_{N_b} + \tilde{\boldsymbol{\Lambda}}\mathbf{1}_{N_b} \stackrel{(5.5)}{=} \mathbf{0}. \tag{5.30}$$

This shows that $(1/\sqrt{N_b})\mathbf{1}_{N_b}$ must be the leading, normalized eigenvector, for the eigenvalue 0. Consequently, we get from (5.25) that

$$B(N_b X) \stackrel{X\to\infty}{\longrightarrow} \frac{1}{N_b}\left[\mathbf{1}_{N_b}^{\mathrm{T}}\boldsymbol{B}_0 - \frac{1}{N_b}\mathbf{1}_{N_b}^{\mathrm{T}}\boldsymbol{\Gamma}^{(1)\mathrm{T}}\boldsymbol{\Gamma}^{-1}\boldsymbol{S}_0\right]\mathbf{1}_{N_b}$$

$$= \frac{1}{N_b}\left[\boldsymbol{B}_0^{\mathrm{T}}\mathbf{1}_{N_b} - \frac{1}{N_b}\boldsymbol{S}_0^{\mathrm{T}}\boldsymbol{\Gamma}^{-1}\boldsymbol{\Gamma}^{(1)}\mathbf{1}_{N_b}\right]\mathbf{1}_{N_b}$$

$$\stackrel{(5.27)}{=} \frac{1}{N_b}\left(\boldsymbol{B}_0^{\mathrm{T}}\mathbf{1}_{N_b} + \boldsymbol{S}_0^{\mathrm{T}}\mathbf{1}_{N_s}\right)\mathbf{1}_{N_b} \approx \frac{R^2}{N}\mathbf{1}_{N_b}, \tag{5.31}$$

where we used that $\boldsymbol{B}_0^{\mathrm{T}}\mathbf{1}_{N_b} + \boldsymbol{S}_0^{\mathrm{T}}\mathbf{1}_{N_s} = \sum_{j=1}^{N}P_j(0) = R^2$ and made the approximation $1/N = 1/(N_b + N_s) \approx 1/N_b$.

Equation (5.31) gives the equipartition of the powers of the body waves, and substituting in (5.26) we get the equipartition of the powers of the surface waves

$$S(N_b X) \stackrel{X\to\infty}{\longrightarrow} -\frac{1}{N_b}\boldsymbol{\Gamma}^{-1}\boldsymbol{\Gamma}^{(1)}\frac{R^2}{N}\mathbf{1}_{N_b} \stackrel{(D1)}{=} \frac{R^2}{N}\mathbf{1}_{N_s}. \tag{5.32}$$

(c) Discussion

The analysis in the previous two sections shows that the mean powers become equidistributed at range $x \gg N_b$, but the dynamics is multi-scale. The powers of the surface waves relax quickly, on a range scale of $O(1)$ and reach a metastable distribution of power that is in general not uniform, and depends on the entries in the off-diagonal block $\boldsymbol{\Gamma}^{(1)}$ in (5.1). Only when the entries in $\boldsymbol{\Gamma}^{(1)}$ are all equal to γ_1 the distribution of power in the metastable state is uniform. This was obtained in §5a and to reach the same conclusion from the expression (5.23) we note from definition (5.4) that for such $\boldsymbol{\Gamma}^{(1)}$ we have $\boldsymbol{\Lambda} = \gamma_1 \mathbf{I}_{N_s}$. Then, the first term in (5.23) is

$$-\frac{1}{N_b}\boldsymbol{\Gamma}^{-1}\boldsymbol{\Gamma}^{(1)}\boldsymbol{B}_0 \stackrel{(5.18)}{=} -\frac{1}{N_b}\left(\boldsymbol{\Gamma}^{(0)} - \boldsymbol{\Lambda}\right)^{-1}\boldsymbol{\Gamma}^{(1)}\boldsymbol{B}_0 = -\frac{1}{N_b}\left(\boldsymbol{\Gamma}^{(0)} - \gamma_1\mathbf{I}_{N_s}\right)^{-1}\gamma_1 R_{b,0}^2\mathbf{1}_{N_s}$$

$$= \frac{R_{b,0}^2}{N_b}\mathbf{1}_{N_s} \approx \frac{R_{b,0}^2}{N}\mathbf{1}_{N_s}, \tag{5.33}$$

where we used that $\boldsymbol{\Gamma}^{(0)}\mathbf{1}_{N_s} = \mathbf{0}$ and therefore $(\boldsymbol{\Gamma}^{(0)} - \gamma_1\mathbf{I}_{N_s})^{-1}\mathbf{1}_{N_s} = -(1/\gamma_1)\mathbf{1}_{N_s}$. The second term in (5.23) is obtained similarly, using the observation that

$$\boldsymbol{\Gamma}^{-1}\boldsymbol{S}_0 = -\frac{R_{s,0}^2}{N_s\gamma_1}\mathbf{1}_{N_s} + \sum_{j=2}^{N_s}(-g_j - \gamma_1)^{-1}\left[\boldsymbol{v}_j^{\mathrm{T}}\boldsymbol{S}_0\right]\boldsymbol{v}_j,$$

where $-g_j$, for $j = 2, \ldots, N_s$ are the non-zero eigenvalues of $\boldsymbol{\Gamma}^{(0)}$ and $\boldsymbol{v}_j$ are the eigenvectors, which are orthogonal to the leading one $(1/\sqrt{N_s})\mathbf{1}_{N_s}$. This implies that

$$\boldsymbol{\Gamma}^{(1)\mathrm{T}}\boldsymbol{v}_j = \mathbf{0}, \qquad j = 2, \ldots, N_s,$$

and the second term in (5.23) becomes

$$\frac{1}{N_b{}^2}\boldsymbol{\Gamma}^{-1}\boldsymbol{\Gamma}^{(1)}\boldsymbol{\Gamma}^{(1)\mathrm{T}}\boldsymbol{\Gamma}^{-1}S_0 = -\frac{R_{s,0}^2}{N_b{}^2 N_s \gamma_1}\boldsymbol{\Gamma}^{-1}\boldsymbol{\Gamma}^{(1)}\boldsymbol{\Gamma}^{(1)\mathrm{T}}\mathbf{1}_{N_s} = -\frac{R_{s,0}^2}{N_b{}^2}\boldsymbol{\Gamma}^{-1}\boldsymbol{\Gamma}^{(1)}\mathbf{1}_{N_b}$$

$$= -\frac{R_{s,0}^2\gamma_1}{N_b}\boldsymbol{\Gamma}^{-1}\mathbf{1}_{N_s} = \frac{R_{s,0}^2}{N_b}\mathbf{1}_{N_s} \approx \frac{R_{s,0}^2}{N}\mathbf{1}_{N_s}. \tag{5.34}$$

We conclude from (5.23), (5.33), (5.34) and (5.26) that in the special case of $\boldsymbol{\Gamma}^{(1)}$ with all entries equal to γ_1 there is a uniform distribution of the surface wave powers at range $1 \ll x \le O(N_b)$, as in §5a.

The body wave powers evolve very slowly, on a range scale $x = O(N_b)$, and while doing so, they affect the powers of the surface waves. At range $x \gg N_b$ the body wave powers become uniformly distributed and this drives the whole system, including the surface waves, to equipartition.

We end the section with the remark that the order of the two limits in our analysis is important. We first let $\varepsilon \to 0$ to derive the radiative transfer equation and then let $kD \to \infty$ i.e. $N_b \to \infty$ to analyse the convergence to equipartition. If we took the limit $kD \to \infty$ first, then the domain would be the half space $(x, z) \in \mathbb{R} \times (-\infty, 0)$, with radiation conditions at $z \to -\infty$. The spectrum of the unperturbed Helmholtz operator in the half space has a discrete part, with the N_s eigenvalues in the interval (k^2, n^2k^2) defined by equation (3.6), and the corresponding eigenvectors given by (3.8) and (3.9) that define the surface waves. However, the body waves are replaced by radiation modes, corresponding to the continuous spectrum in $(0, k^2)$. One can establish [32] a convergence result for the discrete mean surface wave powers that reads

$$\partial_x P_j(x) = \sum_{l=1}^{N_s} \Gamma_{jl}^{(0)} P_l(x) - \Lambda_{jj} P_j(x), \tag{5.35}$$

with $\boldsymbol{\Gamma}^{(0)}$ given by (5.3) and positive definite, diagonal $\boldsymbol{\Lambda}$. We observe from these equations that $\partial_x \sum_{j=1}^{N_s} P_j(x) = -\sum_{j=1}^{N_s} \Lambda_{jj} P_j(x) < 0$, so the power carried by the discrete surface modes leaks to the radiating (body) modes. However, there is no feedback from the radiating modes towards the surface modes in this framework, because the range scale required to get this feedback is beyond that of validity of the convergence result for this system. Such feedback is captured in our setting by the radiative transfer equation (4.14), which conserves the total mean power.

6. Numerical illustrations

We now complement the analysis in §5, carried out in the limit $kD \to \infty$, with numerical simulations for large kD and therefore, large N_b.

In figure 2, we verify the estimates (3.7) and (3.15) of N_s and N_b. We display with the blue solid lines the numbers of the numerically calculated eigenvalues and with the red dashed lines the estimates $kd\sqrt{n^2-1}/\pi$ (plot a) and $k(D-d)/\pi$ (plot b) for N_s and N_b, respectively.

In figure 3, we give the eigenvalues λ_j for $j = 1, \ldots, N_s$ in plots a,c and $j = N_s + 1, \ldots, N$ in plots b,d. These eigenvalues are calculated by solving equations (3.5) and (3.13). In plots a,c, we fix $kD = 100$ and vary kd in the interval $(0, 10)$, for two values of the squared index of refraction: $n^2 = 2$ in the plots a,b and $n^2 = 10$ in plots c,d. As expected from the estimate (3.7), the number N_s of surface waves grows with kd and with n^2. Plots b,d show that the number of body waves increases with kD but it is basically independent of n^2, as expected from the results in §3b.

The remaining figures are for $n^2 = 10$, $kd = 6$ and $kD = 100$, so that the spectrum of the Helmholtz operator $\partial_z^2 + k^2 n_0^2(z)$ is as displayed in figure 4. There are $N_s = 6$ surface waves and $N_b = 30$ body waves. Figure 4b compares the calculated eigenvalues $(\lambda_j)_{j=7}^{36}$ with the approximation (see §3b)

$$\frac{\lambda_j}{k^2} \approx 1 - \frac{(j - N_s - 1/2)^2 \pi^2}{(D-d)^2}, \quad N_s = 6, \ j = 7, \ldots, 36. \tag{6.1}$$
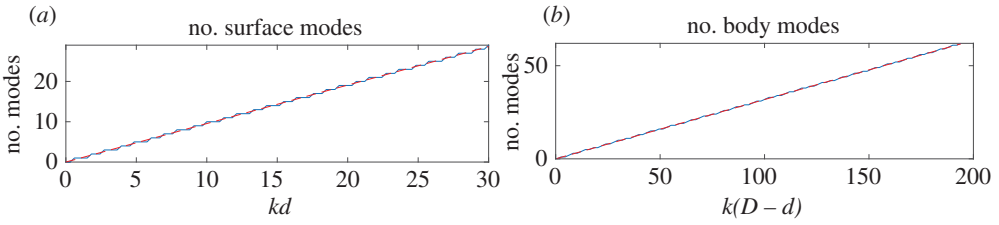
Figure 2. (*a*) N_s versus kd, for $n^2 = 10$ and $kD = 100$. (*b*) N_b versus $k(D - d)$ for $n^2 = 10$ and $kd = 6$. (Online version in colour.)
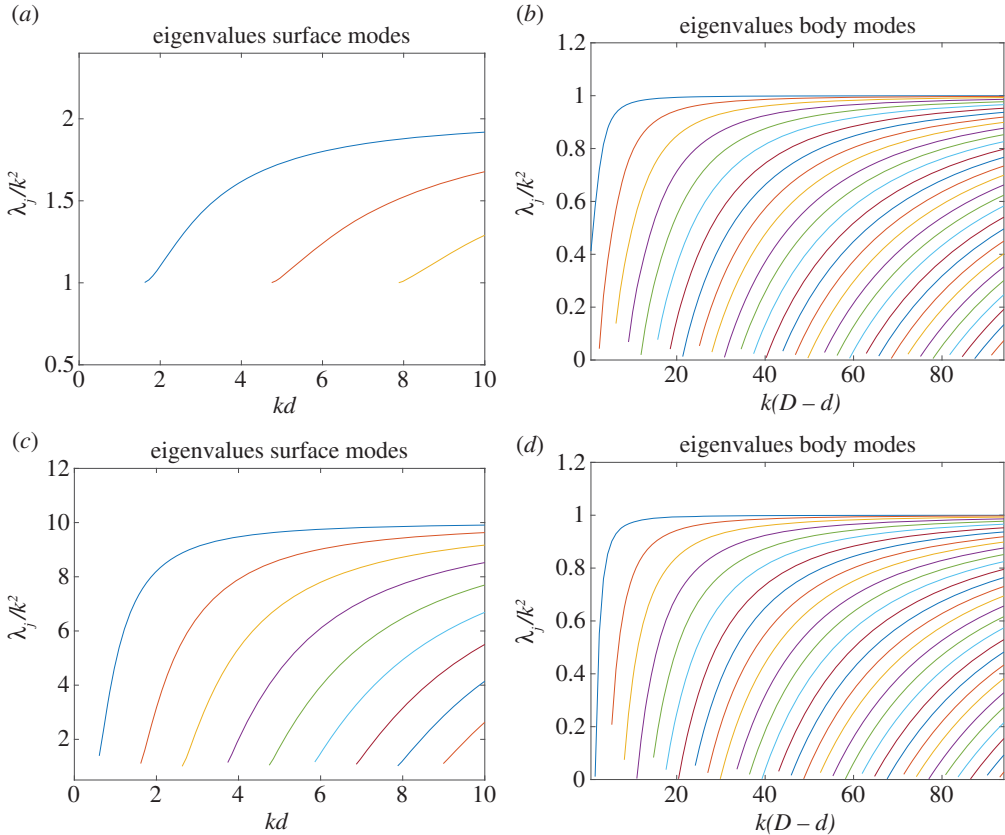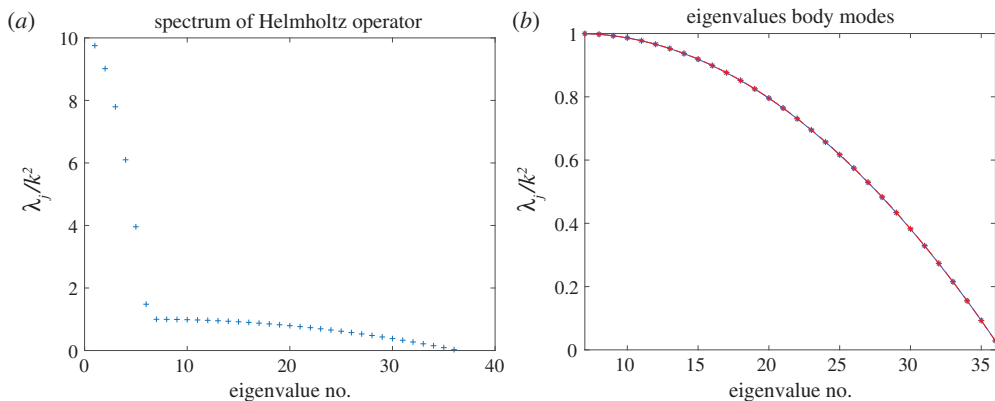

Figure 3. (*a,c*) Eigenvalues in the spectral interval $(k^2, n^2 k^2)$. (*b,d*) Eigenvalues in the spectral interval $(0, k^2)$. Plots (*a,b*) are for $n^2 = 2$ and (*c,d*) plots are for $n^2 = 10$. (Online version in colour.)

To illustrate the evolution towards equipartition, we consider a Gaussian covariance function (2.4) of the fluctuations of the index of refraction in the surface layer

$$
\mathcal{C}(x, z, z') = \exp\left(-\frac{x^2}{2\ell^2} - \frac{(z - z')^2}{2\ell^2}\right),
\tag{6.2}
$$

where ℓ is the correlation length. The entries of $\boldsymbol{\Gamma}^c$ calculated using definitions (4.4) and (4.8) are

$$
\Gamma_{jl}^c = \frac{\sqrt{\pi} k^4 \ell}{2\sqrt{2} \beta_j \beta_l} \exp\left(-\frac{(\beta_l - \beta_j)^2 \ell^2}{2}\right) \int_{-d}^{0} \int_{-d}^{0} \phi_j(z)\phi_l(z) \exp\left(-\frac{(z - z')^2}{2\ell^2}\right) \phi_j(z')\phi_l(z') \, \mathrm{d}z \mathrm{d}z',
$$

Figure 4. (a) Spectrum of the Helmholtz operator for $n^2 = 10$, $kd = 6$ and $kD = 100$. There are six eigenvalues in the spectral interval $(k^2, n^2 k^2)$, corresponding to the surface waves. The remaining 30 eigenvalues in the interval $(0, k^2)$ are compared in plot (b) with the asymptotic expression (6.1) discussed in §3b. (Online version in colour.)
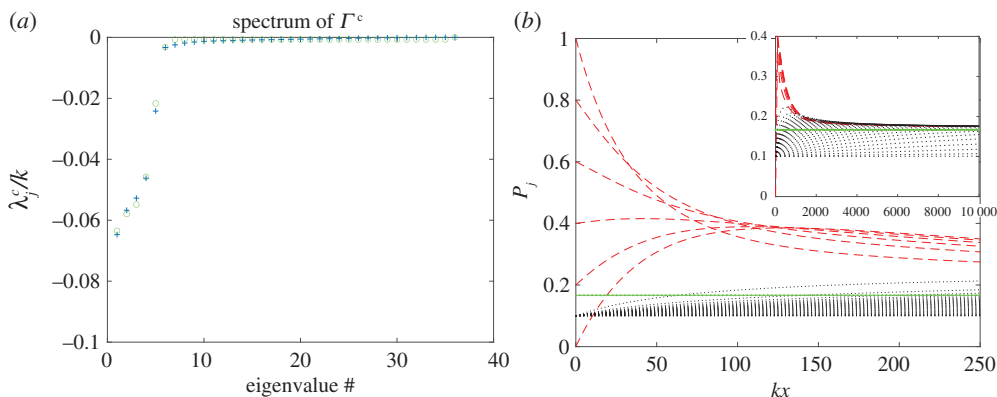
Figure 5. Results for the Gaussian covariance with $\ell = 1/k$. (a) The eigenvalues λ_j^ς of $\boldsymbol{\Gamma}^c$ are shown with blue crosses and the estimates $\lambda_j^\varsigma = \theta_{N+1-j}$ with θ_j given by (6.3) are shown with the green circles. (b) Evolution of the mode powers with increasing range x. The surface mode powers are shown with red dashed lines, the body mode powers are shown with black dotted lines, and the solid green line is the average mode power. The inset corresponds to longer propagation distances (kx up to 10^4) and displays the evolution toward equipartition, albeit very slowly for the body modes. (Online version in colour.)

and they have a non-monotone dependence with respect to the correlation length ℓ. Note that the entries Γ_{jl}^c are large when ℓ is somewhat larger than $1/k$, so that the factor $\ell \exp(-(\beta_j - \beta_l)^2 \ell^2/2)$ is large, also that the entries tend to zero when ℓ goes to zero or infinity. In figure 5a, we show with blue crosses the eigenvalues λ_j^c of $\boldsymbol{\Gamma}^c$ and with green circles the eigenvalues $\lambda_j^c = \theta_{N+1-j}$ given in §5a for the simplified model (5.7) and (5.8) by

$$
\theta_j =
\begin{cases}
0, & \text{if } j = 1, \\
-\dfrac{(\gamma_2 + \gamma_1 N_s)}{N_b}, & \text{if } j = 2, \ldots, N_b, \\
-\gamma_1 \left(1 + \dfrac{N_s}{N_b}\right) & \text{if } j = N_b + 1, \\
-(g_j + \gamma_1) & \text{if } j = N_b + 2, \ldots, N,
\end{cases}
\tag{6.3}
$$

where $-g_j$ are the eigenvalues of $\boldsymbol{\Gamma}^{(0)}$ and the constants γ_1, γ_2 are taken to be the averaged values of the entries of the block matrices:

$$\gamma_1 = \frac{1}{N_s} \sum_{j=1}^{N_s} \sum_{l=1}^{N_b} \Gamma_{jl}^c \quad \text{and} \quad \gamma_2 = \frac{2N_b}{(N_b - 1)} \sum_{j,l=N_s+1}^{N} \Gamma_{jl}^c.$$

Note that even though the entries in the blocks $\boldsymbol{\Gamma}^{(1)}$ and $\boldsymbol{\Gamma}^{(2)}$ of $\boldsymbol{\Gamma}^c$ have O(1) relative variations, the model in §5a gives good estimates of the eigenvalues.

Figure 5b, we display the evolution of the mode powers with range. The surface mode powers are shown with red dashed lines and the body wave powers with black dotted lines. The average mode power or equipartition limit R^2/N is shown with the green solid line. As predicted by the theory, we see a rapid relaxation of the surface wave powers that lasts up to the scaled range $kx \approx 50$, after which there is a slow transition towards equipartition. The body mode powers evolve very slowly, as predicted by the analysis.

7. Summary

We introduced a mathematical model for studying the transfer of power between surface and body waves as they transition towards the equilibrium state of equipartition of power. The model is a two-dimensional acoustic waveguide in the domain $(x, z) \in \mathbb{R} \times (-D, 0)$. The waveguide has reflecting boundaries at $z = 0$ and $z = -D$, and a thin 'surface' layer of width $d \ll D$, adjacent to the top boundary. This layer is filled with a weakly inhomogeneous random medium, whereas the remainder of the waveguide is filled with a homogeneous medium. There are two kinds of wave modes in the waveguide: those that propagate and those that decay i.e. are evanescent. The propagating modes can be classified further as those that are trapped in the surface layer, and thus model surface waves, and those that penetrate in the entire cross section of the waveguide and model body waves.

We use asymptotic stochastic analysis to study from first principles the coupling between the propagating and the evanescent modes induced by scattering in the surface layer, and derive a radiative transfer equation for the mean powers of the propagating modes. With this equation we study the evolution of the mode powers in the asymptotic regime $kD \to \infty$. This corresponds to having a finite number of surface waves and an infinite number of body waves. We prove the convergence of the mean mode powers to the equilibrium state of equipartition and show that the dynamics during this convergence is multi-scale: the surface wave powers evolve quickly, and reach a metastable state that changes slowly due to the back and forth transfer of power with the body waves. The body wave powers evolve very slowly and eventually reach equipartition. When this happens, the whole system, including the surface waves, is in the equipartition state, i.e. the power is distributed uniformly over the modes.

The model presented in this paper seeks to mimic seismic wave propagation in the Earth's crust, which is much more complex due to the presence of different types of surface waves such as Rayleigh and Love waves. It is a first step towards the full understanding of radiative transfer in seismology. The next step should be to incorporate polarization effects for elastic waves (this was done in open media in [17]). Another important point would be to take into account energy absorption, which is expected to affect surface waves because of the presence of fluids in the sub-surface of the Earth.

Appendix A. Proof of the statements in §3a

We begin with the proof that the number of solutions of equation (3.6) in the spectral interval (k^2, k^2n^2) is N_s defined by (3.7).

Proof. λ is a solution in (k^2, n^2k^2) of (3.6) if and only if $t = d\sqrt{k^2n^2 - \lambda}$ is a solution in $\left(0, kd\sqrt{n^2 - 1}\right)$ of $\psi(t) = \tan(t)$, where the function

$$\psi(t) = -\frac{t}{\sqrt{k^2d^2(n^2 - 1) - t^2}} \tag{A 1}$$

is a monotonically decreasing function from $\left(0, kd\sqrt{n^2 - 1}\right)$ onto $(-\infty, 0)$, with $\lim_{t \nearrow kd\sqrt{n^2-1}} \psi(t) = -\infty$, as shown in figure 6. We look for the solutions $t \in \left(0, kd\sqrt{n^2 - 1}\right)$ of $\psi(t) = \tan(t)$:

— There is no solution in $(0, \pi/2)$ because $\tan(t) > 0$ and $\psi(t) < 0$. There is exactly one solution in $(\pi/2, \pi)$ iff $kd\sqrt{n^2 - 1} > \pi/2$, otherwise there is no solution.
— For any positive integer p: There is no solution in $(p\pi, (p + 1/2)\pi)$ because $\tan(t) > 0$ and $\psi(t) < 0$ and there is exactly one solution in $((p + 1/2)\pi, (p + 1)\pi)$ iff $kd\sqrt{n^2 - 1} > (p + 1/2)\pi$. Otherwise there is no solution. Consequently, the number N_s of solutions is the unique integer such that $(N_s - 1/2)\pi < kd\sqrt{n^2 - 1} \le (N_s + 1/2)\pi$. This completes the proof of (3.7). ∎

Now let us describe the eigenfunctions that define the surface waves, which are defined in equations (3.3) and (3.4) for a finite D,

$$\phi_j(z) = \begin{cases} A_j \sin\left[\sqrt{k^2n^2 - \lambda_j}\, z\right], & \text{if } z \in (-d, 0), \\ -A_j \sin\left[\sqrt{k^2n^2 - \lambda_j}\, d\right] \dfrac{\cosh\left[\sqrt{\lambda_j - k^2}\, (D + z)\right]}{\cosh\left[\sqrt{\lambda_j - k^2}\, (D - d)\right]}, & \text{if } z \in (-D, -d). \end{cases} \tag{A 2}$$

Rewriting the ratio of the cosh functions we obtain that

$$\frac{\cosh\left[\sqrt{\lambda_j - k^2}\,(D + z)\right]}{\cosh\left[\sqrt{\lambda_j - k^2}\,(D - d)\right]} = \frac{\exp\left[\sqrt{\lambda_j - k^2}\,(z + d)\right] + \exp\left[-\sqrt{\lambda_j - k^2}\,(2D + z - d)\right]}{1 + \exp\left[-\sqrt{\lambda_j - k^2}\,(2D - 2d)\right]}$$
$$\approx \exp\left[\sqrt{\lambda_j - k^2}\,(z + d)\right],$$

where the approximation is for $kD \gg 1$. The expression (3.8) of the eigenfunctions follows in the limit $kD \to \infty$.

It remains to compute the normalizing constant A_j. Direct integration gives

$$1 = \int_{-\infty}^{0} \phi_j^2(z)\,dz = \frac{A_j^2}{2}\left[d - \frac{\sin\left[d\sqrt{k^2n^2 - \lambda_j}\right]\cos\left[d\sqrt{k^2n^2 - \lambda_j}\right]}{\sqrt{k^2n^2 - \lambda_j}} + \frac{\sin^2\left[d\sqrt{k^2n^2 - \lambda_j}\right]}{\sqrt{\lambda_j - k^2}}\right]$$

$$\overset{(3.6)}{=} \frac{A_j^2}{2}\left[d + \frac{\cos^2\left[d\sqrt{k^2n^2 - \lambda_j}\right]}{\sqrt{\lambda_j - k^2}} + \frac{\sin^2\left[d\sqrt{k^2n^2 - \lambda_j}\right]}{\sqrt{\lambda_j - k^2}}\right] = \frac{A_j^2}{2}\left[d + \frac{1}{\sqrt{\lambda_j - k^2}}\right],$$

as stated in equation (3.9).
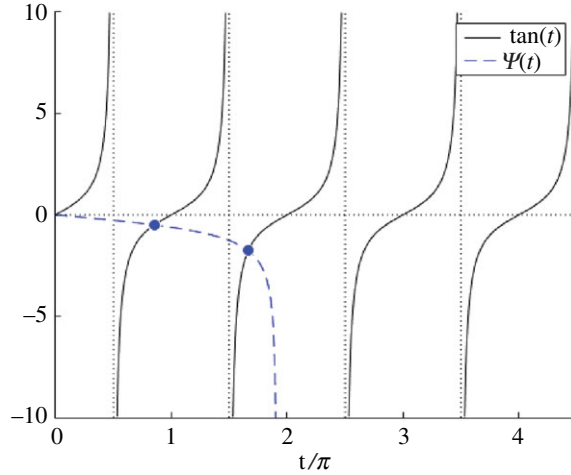
Figure 6. Determination of the solutions of the equation $\psi(t) = \tan(t)$ with $kd\sqrt{n^2 - 1} = 6$. Here there are $N_s = 2$ solutions (the blue dots). (Online version in colour.)

Appendix B. Proof of the statements in §3b

To estimate the number of body waves in the regime $kD \gg 1$, note that in equation (3.13) only $\tan[(D - d)\sqrt{k^2 - \lambda}]$ varies rapidly in λ. The remaining factors are approximately constant over a period of this tangent.

Let λ_j and λ_{j+1} be two consecutive solutions of (3.13), and define

$$\bar{\lambda} := \frac{\lambda_j + \lambda_{j+1}}{2}, \qquad \widetilde{\lambda} := \lambda_j - \lambda_{j+1} > 0. \tag{B1}$$

Using the observation above, we conclude that

$$D\sqrt{k^2 - \lambda_{j+1}} - D\sqrt{k^2 - \lambda_j} = D\sqrt{k^2 - \bar{\lambda} + \frac{\widetilde{\lambda}}{2}} - D\sqrt{k^2 - \bar{\lambda} - \frac{\widetilde{\lambda}}{2}} \approx \pi. \tag{B2}$$

Squaring this equation and rearranging terms: $\sqrt{(k^2 - \bar{\lambda})^2 - \widetilde{\lambda}^2/4} \approx k^2 - \bar{\lambda} - \pi^2/(2D^2)$. Squaring one more time and solving for $\widetilde{\lambda}$,

$$\widetilde{\lambda} \approx \frac{2\pi}{D}\sqrt{k^2 - \bar{\lambda}}\left[1 + \frac{\pi^2}{4D^2(k^2 - \bar{\lambda})}\right] \approx \frac{2\pi}{D}\sqrt{k^2 - \bar{\lambda}}. \tag{B3}$$

This shows that the separation between the eigenvalues is approximately inverse proportional to D, and in combination with (B1) it leads to the recursion relation

$$\lambda_j - \lambda_{j+1} \approx \frac{2\pi}{D}\sqrt{k^2 - \lambda_j}, \tag{B4}$$

stated in §3b.

We estimate the normalizing constant A_j of $\phi_j(z)$ using (3.10)

$$
\begin{aligned}
1 = \int_{-D}^{0} \phi_j^2(z)\,dz = A_j^2 &\left\{ \frac{(D-d)}{2} \frac{\sin^2\left[d\sqrt{k^2n^2 - \lambda_j}\right]}{\cos^2\left[(D-d)\sqrt{k^2 - \lambda_j}\right]} + \frac{d}{2} - \frac{1}{4}\sin\left[2d\sqrt{k^2n^2 - \lambda_j}\right] \right. \\
&\left. \times \left[\frac{\tan\left[d\sqrt{k^2n^2 - \lambda_j}\right]\tan\left[(D-d)\sqrt{k^2 - \lambda_j}\right]}{\sqrt{k^2 - \lambda_j}} - \frac{1}{\sqrt{k^2n^2 - \lambda_j}} \right] \right\} \\
\overset{(3.13)}{=} A_j^2 &\left[\frac{(D-d)}{2} \frac{\sin^2\left[d\sqrt{k^2n^2 - \lambda_j}\right]}{\cos^2\left[(D-d)\sqrt{k^2 - \lambda_j}\right]} + \frac{d}{2} - \frac{\sin\left[2d\sqrt{k^2n^2 - \lambda_j}\right]k^2(n^2-1)}{4(k^2 - \lambda_j)\sqrt{k^2n^2 - \lambda_j}} \right] \\
\approx & \frac{A_j^2 D \sin^2\left[d\sqrt{k^2n^2 - \lambda_j}\right]}{2\cos^2\left[(D-d)\sqrt{k^2 - \lambda_j}\right]}.
\end{aligned}
$$

This gives that

$$
A_j^2 \approx \frac{2\cos^2\left[(D-d)\sqrt{k^2 - \lambda_j}\right]}{D\sin^2\left[d\sqrt{k^2n^2 - \lambda_j}\right]}, \tag{B5}
$$

and therefore, by (3.11), $B_j^2 \approx 2/D$. Finally, we rewrite further equation (B 5) using equation (3.13):

$$
\begin{aligned}
A_j^2 &\approx \frac{2\cos^2\left[(D-d)\sqrt{k^2 - \lambda_j}\right]}{D\sin^2\left[d\sqrt{k^2n^2 - \lambda_j}\right]} = \frac{2}{D\sin^2\left[d\sqrt{k^2n^2 - \lambda_j}\right]\left[1 + \tan^2\left[(D-d)\sqrt{k^2 - \lambda_j}\right]\right]} \\
&\overset{(3.13)}{=} \frac{2}{D\left[\sin^2\left[d\sqrt{k^2n^2 - \lambda_j}\right] + \frac{(k^2n^2 - \lambda_j)}{(k^2 - \lambda_j)}\cos^2\left[d\sqrt{k^2n^2 - \lambda_j}\right] \right]} \\
&= \frac{2(k^2 - \lambda_j)}{D\left[k^2 - \lambda_j + k^2(n^2 - 1)\cos^2\left[d\sqrt{k^2n^2 - \lambda_j}\right]\right]}, \tag{B6}
\end{aligned}
$$

as stated in §3b.

Appendix C. Estimation of the mean mode powers

Let us begin with the observation that the negative definite diagonal blocks $\boldsymbol{\Gamma}$ and $\widetilde{\boldsymbol{\Gamma}}$ satisfy

$$
\exp\left(\boldsymbol{\Gamma} x\right) \approx 0, \quad \text{for } x \gg 1, \tag{C1}
$$

$$
\exp\left(\widetilde{\boldsymbol{\Gamma}}\,\frac{x}{N_b}\right) = \mathbf{I}_{N_b} + O\left(\frac{x}{N_b}\right), \quad \text{for } 0 < x \ll N_b, \tag{C2}
$$

$$
\exp\left(\widetilde{\boldsymbol{\Gamma}}\,\frac{x}{N_b}\right) \to 0, \quad \text{for } \frac{x}{N_b} \to \infty. \tag{C3}
$$

In the next two sections, we use these results to estimate the mean mode powers in two distinct range intervals: $x \ll N_b$ and $x = O(N_b)$.

(a) Estimates at range $x \ll N_b$

Let us iterate once equations (5.19) and (5.20) and use a change of variable of integration, to obtain

$$S(x) = \exp\left(\boldsymbol{\Gamma} x\right) S_0 + \frac{1}{N_b} \int_0^x \exp\left(\boldsymbol{\Gamma} x'\right) \boldsymbol{\Gamma}^{(1)} \exp\left(\widetilde{\boldsymbol{\Gamma}} \frac{x - x'}{N_b}\right) B_0 \, dx'$$

$$+ \frac{1}{N_b{}^2} \int_0^x \left[\int_{x'}^x \exp\left(\boldsymbol{\Gamma}(x - x'')\right) \boldsymbol{\Gamma}^{(1)} \exp\left(\widetilde{\boldsymbol{\Gamma}} \frac{x'' - x'}{N_b}\right) dx'' \right] \boldsymbol{\Gamma}^{(1)\mathrm{T}} S(x') \, dx', \qquad (C\,4)$$

and

$$B(x) = \exp\left(\widetilde{\boldsymbol{\Gamma}} \frac{x}{N_b}\right) B_0 + \frac{1}{N_b} \int_0^x \exp\left(\widetilde{\boldsymbol{\Gamma}} \frac{x'}{N_b}\right) \boldsymbol{\Gamma}^{(1)\mathrm{T}} \exp\left(\boldsymbol{\Gamma}(x - x')\right) S_0 \, dx'$$

$$+ \frac{1}{N_b{}^2} \int_0^x \left[\int_{x'}^x \exp\left(\widetilde{\boldsymbol{\Gamma}} \frac{(x - x'')}{N_b}\right) \boldsymbol{\Gamma}^{(1)\mathrm{T}} \exp\left(\boldsymbol{\Gamma}(x'' - x')\right) dx'' \right] \boldsymbol{\Gamma}^{(1)} B(x') \, dx'. \qquad (C\,5)$$

We now use these equations to approximate the vectors $S(x)$ and $B(x)$ of the mean mode powers, as we increase the range x.

We begin with the estimation of $S(x)$: For $x \ll N_b$, we can replace $\exp(\widetilde{\boldsymbol{\Gamma}} \frac{x}{N_b})$ by $\mathbf{I}_{N_b}$ and equation (C 4) gives

$$S(x) = \exp\left(\boldsymbol{\Gamma} x\right) S_0 + \frac{1}{N_b} \left[\int_0^x \exp\left(\boldsymbol{\Gamma} x'\right) dx' \right] \boldsymbol{\Gamma}^{(1)} B_0$$

$$+ \frac{1}{N_b{}^2} \int_0^x \left[\int_{x'}^x \exp\left(\boldsymbol{\Gamma}(x - x'')\right) dx'' \right] \boldsymbol{\Gamma}^{(1)} \boldsymbol{\Gamma}^{(1)\mathrm{T}} S(x') \, dx' + o\left(\frac{R^2}{N_b}\right), \qquad (C\,6)$$

and integrating the exponentials of $\boldsymbol{\Gamma}$ we get

$$S(x) = \exp\left(\boldsymbol{\Gamma} x\right) S_0 + \frac{1}{N_b} \boldsymbol{\Gamma}^{-1} \left[\exp\left(\boldsymbol{\Gamma} x\right) - \mathbf{I}_{N_s} \right] \boldsymbol{\Gamma}^{(1)} B_0$$

$$+ \frac{1}{N_b{}^2} \boldsymbol{\Gamma}^{-1} \int_0^x \left[\exp\left(\boldsymbol{\Gamma}(x - x')\right) - \mathbf{I}_{N_s} \right] \boldsymbol{\Gamma}^{(1)} \boldsymbol{\Gamma}^{(1)\mathrm{T}} S(x') \, dx' + o\left(\frac{R^2}{N_b}\right). \qquad (C\,7)$$

Note that since $\boldsymbol{\Gamma}^{(1)}$ is an $N_s \times N_b$ matrix with $O(1)$ entries, $\boldsymbol{\Gamma}^{(1)} \boldsymbol{\Gamma}^{(1)\mathrm{T}}$ is an $N_s \times N_s$ matrix with $O(N_b)$ entries. Moreover, the vector $\boldsymbol{\Gamma}^{(1)} B_0 \in \mathbb{R}^{N_s}$ has $O(R_{b,0}^2)$ entries by (4.16). Thus, the first term in the right-hand side of (C 7) is $O(R^2)$ and the last two terms are of order $O(R^2/N_b)$. Iterating equation (C 7) one time, and using that $\boldsymbol{\Gamma}^{-1}$ commutes with the exponential of $\boldsymbol{\Gamma}$, we obtain equation (5.21).

When we let $1 \ll x \ll N_b$ in (5.21), and recall that $\boldsymbol{\Gamma}$ is negative definite, we observe that $\exp(\boldsymbol{\Gamma} x)$ goes to zero and the leading-order term involving S_0 is $\frac{1}{N_b{}^2} \boldsymbol{\Gamma}^{-1} \boldsymbol{\Gamma}^{(1)} \boldsymbol{\Gamma}^{(1)\mathrm{T}} \boldsymbol{\Gamma}^{-1} S_0$. The leading-order term involving B_0 is $-\frac{1}{N_b} \boldsymbol{\Gamma}^{-1} \boldsymbol{\Gamma}^{(1)} B_0$. We then get from (5.21) that

$$S(x) = -\frac{1}{N_b} \boldsymbol{\Gamma}^{-1} \boldsymbol{\Gamma}^{(1)} B_0 + \frac{1}{N_b{}^2} \boldsymbol{\Gamma}^{-1} \boldsymbol{\Gamma}^{(1)} \boldsymbol{\Gamma}^{(1)\mathrm{T}} \boldsymbol{\Gamma}^{-1} S_0 + o\left(\frac{R^2}{N_b}\right), \quad \text{for } 1 \ll x \ll N_b, \qquad (C\,8)$$

where the first term is $O(R^2)$, the second term is $O(R^2/N_b)$ and the residual tends to zero faster than R^2/N_b in the limit $N_b \to \infty$.

For the vector of mean mode powers of the body waves at range $x \ll N_b$, we can approximate the second and third exponentials of $\widetilde{\boldsymbol{\Gamma}}$ in (C 5) by the identity $\mathbf{I}_{N_b}$ and obtain

$$B(x) = \exp\left(\widetilde{\boldsymbol{\Gamma}} \frac{x}{N_b}\right) B_0 + \frac{1}{N_b} \boldsymbol{\Gamma}^{(1)\mathrm{T}} \boldsymbol{\Gamma}^{-1} \left[\exp\left(\boldsymbol{\Gamma} x\right) - \mathbf{I}_{N_s} \right] S_0 + o\left(\frac{R^2}{N_b}\right), \qquad (C\,9)$$

which is equation (5.22). The first term in the right-hand side is $O(R^2)$ and the second term is $O(R^2/N_b)$. Finally, at $1 \ll x \ll N_b$ the approximation becomes

$$B(x) = \exp\left(\widetilde{\boldsymbol{\Gamma}} \frac{x}{N_b}\right) B_0 - \frac{1}{N_b} \boldsymbol{\Gamma}^{(1)\mathrm{T}} \boldsymbol{\Gamma}^{-1} S_0 + o\left(\frac{R^2}{N_b}\right). \qquad (C\,10)$$

(b) Estimates at range $x = O(N_b)$

Let us set $x = N_b X$, with $X = O(1)$, and use (C 1) in (5.19) to obtain

$$S(N_b X) \approx \frac{1}{N_b} \int_0^{N_b X} \exp(\Gamma x') \Gamma^{(1)} B(N_b X - x') \, dx'. \tag{C 11}$$

Due to the decaying exponential, only ranges $x' = O(1)$ contribute to the integral, and we can use the expansion $B(N_b X - x') \approx B(N_b X) + O(R^2/N_b)$, where the remainder is because, by (5.20), $\partial_x B(x) = O(R^2/N_b)$. Therefore, we get the expression

$$S(N_b X) \approx \frac{1}{N_b} \int_0^{N_b X} \exp(\Gamma x') \, dx' \, \Gamma^{(1)} B(N_b X)$$

$$= \frac{1}{N_b} \Gamma^{-1} \big[\exp(\Gamma N_b X) - I_{N_s} \big] \Gamma^{(1)} B(N_b X) \approx -\frac{1}{N_b} \Gamma^{-1} \Gamma^{(1)} B(N_b X). \tag{C 12}$$

The body wave powers satisfy the ordinary differential equation

$$\partial_X B(N_b X) = \widetilde{\Gamma} B(N_b X) + \Gamma^{(1)\mathrm{T}} S(N_b X) \overset{(\mathrm{C\,12})}{\approx} \left[\widetilde{\Gamma} - \frac{1}{N_b} \Gamma^{(1)\mathrm{T}} \Gamma^{-1} \Gamma^{(1)} \right] B(N_b X). \tag{C 13}$$

Then with the initial condition deriving from (C 10) with $0 < X \ll 1$, we find

$$B(N_b X) \approx \exp\left[\left(\widetilde{\Gamma} - \frac{1}{N_b} \Gamma^{(1)\mathrm{T}} \Gamma^{-1} \Gamma^{(1)} \right) X \right] \left[B_0 - \frac{1}{N_b} \Gamma^{(1)\mathrm{T}} \Gamma^{-1} S_0 \right],$$

and substituting into (C 12) we get that

$$S(N_b X) \approx -\frac{1}{N_b} \Gamma^{-1} \Gamma^{(1)} \exp\left[\left(\widetilde{\Gamma} - \frac{1}{N_b} \Gamma^{(1)\mathrm{T}} \Gamma^{-1} \Gamma^{(1)} \right) X \right] \left[B_0 - \frac{1}{N_b} \Gamma^{(1)\mathrm{T}} \Gamma^{-1} S_0 \right].$$

Appendix D. Identities needed in the convergence analysis

To derive identity (5.27), let us obtain from definition (5.4) of the diagonal matrix Λ that

$$\frac{1}{N_b} \Gamma^{(1)} \mathbf{1}_{N_b} = \Lambda \mathbf{1}_{N_s}. \tag{D 1}$$

This gives $(1/N_b) \Gamma^{-1} \Gamma^{(1)} \mathbf{1}_{N_b} = \Gamma^{-1} \Lambda \mathbf{1}_{N_s}$, and using that $\Lambda \overset{(5.18)}{=} \Gamma^{(0)} - \Gamma$, we get

$$\frac{1}{N_b} \Gamma^{-1} \Gamma^{(1)} \mathbf{1}_{N_b} = \Gamma^{-1} \Gamma^{(0)} \mathbf{1}_{N_s} - \Gamma^{-1} \Gamma \mathbf{1}_{N_s} = -\mathbf{1}_{N_s}, \tag{D 2}$$

where the last equation is because the rows of $\Gamma^{(0)}$ sum to 0. This proves (5.27).

Identity (5.29) follows from this result and the definition (5.6) of $\widetilde{\Lambda}$,

$$\frac{1}{N_b} \Gamma^{(1)\mathrm{T}} \Gamma^{-1} \Gamma^{(1)} \mathbf{1}_{N_b} \overset{(\mathrm{D\,2})}{=} -\Gamma^{(1)\mathrm{T}} \mathbf{1}_{N_s} \overset{(5.6)}{=} -\widetilde{\Lambda} \mathbf{1}_{N_b}. \tag{D 3}$$

References

1. Margerin L. 2005 Introduction to radiative transfer of seismic waves. In *Seismic earth: array analysis of broadband seismograms* (eds A Levander and G. Nolet). Geophysical Monograph Series, vol. 157. Washington, DC: American Geophysical Union.
2. Snieder R. 2002 Scattering of surface waves. In *Scattering and inverse scattering in pure and applied sciences* (eds R Pike, P Sabatier), ch. 1.7.3, pp. 562–577. New York, NY: Academic Press.
3. Vanlanduit S, Guillaume P, Van Der Linden G. 2003 On-line monitoring of fatigue cracks using ultrasonic surface waves. *NDT & E Int.* **36**, 601–607. (doi:10.1016/S0963-8695(03) 00082-3)
4. Chaplain GJ *et al.* 2020 Tailored elastic surface to body wave Umklapp conversion. *Nat. Commun.* **11**, 1–6. (doi:10.1038/s41467-020-17021-x)

5. Seshadri SR. 1993 Leaky Rayleigh waves. *J. Appl. Phys.* **73**, 3637–3650. (doi:10.1063/1.352922)

6. Chandrasekar S. 1960 *Radiative transfer*. New York, NY: Dover Publications.

7. Sato H, Fehler MC, Maeda T. 2012 *Seismic wave propagation and scattering in the heterogeneous earth*. Berlin, Germany: Springer.

8. Trégourès NP, van Tiggelen BA. 2002 Quasi-two-dimensional transfer of elastic waves. *Phys. Rev. E* **66**, 036601. (doi:10.1103/PhysRevE.66.036601)

9. Wu RS. 1985 Multiple scattering and energy transfer of seismic waves - separation of scattering effect from intrinsic attenuation I. *Theor. Model.* **82**, 57–80. (doi:10.1111/j.1365-246X.1985.tb05128.x)

10. Arridge SR, Schotland JC. 2009 Optical tomography: forward and inverse problems. *Inverse Prob.* **25**, 123010. (doi:10.1088/0266-5611/25/12/123010)

11. Apresyan LA, Kravtsov YA. 1995 *Radiation transfer: statistical and wave aspects*. Amsterdam, The Netherlands: Gordon and Breach.

12. Ishimaru A. 1978 *Wave propagation and scattering in random media*. New York, NY: Academic Press.

13. Bal G, Komorowski T, Ryzhik L. 2010 Kinetic limits for waves in a random medium. *Kinetic & Related Models* **3**, 529–644. (doi:10.3934/krm.2010.3.529)

14. Borcea L, Garnier J. 2016 Polarization effects for electromagnetic wave propagation in random media. *Wave Motion* **63**, 179–208. (doi:10.1016/j.wavemoti.2016.02.006)

15. Borcea L, Garnier J. 2016 Derivation of a one-way radiative transfer equation in random media. *Phys. Rev. E* **93**, 022115. (doi:10.1103/PhysRevE.93.022115)

16. Garnier J, Sølna K. 2009 Coupled paraxial wave equations in random media in the white-noise regime. *Ann. Appl. Probab.* **19**, 318–346. (doi:10.1214/08-AAP543)

17. Ryzhik L, Papanicolaou G, Keller JB. 1996 Transport equations for elastic and other waves in random media. *Wave Motion* **24**, 327–370. (doi:10.1016/S0165-2125(96)00021-2)

18. Maeda T, Sato H, Nishimura T. 2008 Synthesis of coda wave envelopes in randomly inhomogeneous elastic media in a half-space: single scattering model including Rayleigh waves. *Geophys. J. Int.* **172**, 130–154. (doi:10.1111/j.1365-246X.2007.03603.x)

19. Margerin L, Bajaras A, Campillo M. 2019 A scalar radiative transfer model including the coupling between surface and body waves. *Geophys. J. Int.* **219**, 1092–1108. (doi:10.1093/gji/ggz348)

20. Zeng Y. 2006 Scattered surface wave energy in the seismic coda. *Pure Appl. Geophys.* **163**, 533–548. (doi:10.1007/s00024-005-0025-7)

21. Poupinet G, Ellsworth WL, Frechet J. 1984 Monitoring velocity variations in the crust using earthquake doublets: an application to the Calaveras Fault, California. *J. Geophys. Res. Solid Earth* **89**(B7), 5719–5731. (doi:10.1029/JB089iB07p05719)

22. Snieder R, Grêt A, Douma H, Scales J. 2002 Coda wave interferometry for estimating nonlinear behavior in seismic velocity. *Science* **295**, 2253–2255. (doi:10.1126/science.1070015)

23. Sens-Schönfelder C, Larose E. 2008 Temporal changes in the lunar soil from correlation of diffuse vibrations. *Phys. Rev. E* **78**, 045601. (doi:10.1103/PhysRevE.78.045601)

24. Sens-Schönfelder C, Wegler U. 2006 Passive image interferometry and seasonal variations of seismic velocities at Merapi Volcano, Indonesia. *Geophys. Res. Lett.* **33**, L21302. (doi:10.1029/2006GL027797)

25. Campillo M, Paul A. 2003 Long-range correlations in the diffuse seismic coda. *Science* **299**, 547–549. (doi:10.1126/science.1078551)

26. Garnier J, Sølna K. 2011 Background velocity estimation by cross correlations of ambient noise signals in radiative transport regime. *Commun. Math. Sci.* **9**, 743–766. (doi:10.4310/CMS.2011.v9.n3.a5)

27. Lobkis OI, Weaver RL. 2001 On the emergence of the Green's function in the correlations of a diffuse field. *J. Acoust. Soc. Am.* **110**, 3011–3017. (doi:10.1121/1.1417528)

28. Malcolm AE, Scales JA, van Tiggelen BA. 2004 Extracting the Green function from diffuse, equipartitioned waves. *Phys. Rev. E* **70**, 015601. (doi:10.1103/PhysRevE.70.015601)

29. Hennino R, Trégourès N, Shapiro NM, Margerin L, Campillo M, van Tiggelen B, Weaver RL. 2001 Observation of equipartition of seismic waves. *Phys. Rev. Lett.* **86**, 3447–3450. (doi:10.1103/PhysRevLett.86.3447)

30. Weaver RL. 1982 On diffuse waves in solid media. *J. Acoust. Soc. Am.* **71**, 1608–1609. (doi:10.1121/1.387816)

31. Obermann A, Planès TT, Hadziioannou C, Campillo M. 2016 Lapse-time-dependent coda-wave depth sensitivity to local velocity perturbations in 3-D heterogeneous elastic media. *Geophys. J. Int.* **207**, 59–66. (doi:10.1093/gji/ggw264)
32. Garnier J. 2020 Intensity fluctuations in random waveguides. *Commun. Math. Sci.* **18**, 947–971. (doi:10.4310/CMS.2020.v18.n4.a3)
33. Fouque J-P, Garnier J, Papanicolaou G, Sølna K. 2007 *Wave propagation and time reversal in randomly layered media*. New York, NY: Springer.
34. Alonso R, Borcea L, Garnier J. 2012 Wave propagation in waveguides with rough boundaries. *Commun. Math. Sci.* **11**, 233–267. (doi:10.4310/CMS.2013.v11.n1.a7)
35. Garnier J, Papanicolaou G. 2007 Pulse propagation and time reversal in random waveguides. *SIAM J. Appl. Math.* **67**, 1718–1739. (doi:10.1137/060659235)

28

royalsocietypublishing.org/journal/rspa *Proc. R. Soc. A* **477**: 20200775